Effect of Cadherin-13 inactivation on different GABAergic interneuron populations of the mouse hippocampus

Effekt der Cadherin-13 Inaktivierung auf verschiedene GABAerge Interneuronenpopulationen im Hippocampus der Maus

Doctoral thesis for a medical doctoral degree
at the Graduate School of Life Sciences,
Julius-Maximilians-Universität Würzburg,
Section Neuroscience

submitted by

Lucas Bacmeister

from

Hamburg

Würzburg, 2018

Submitted on: …………………………………………………..……..

Members of the Thesis Committee:

Chairperson: **Prof. Dr. Philip Tovote**

Primary Supervisor: **Prof. Dr. Klaus-Peter Lesch**

Supervisor (Second):   **Prof. Dr. Esther Asan**

Supervisor (Third):   **Prof. Dr. Erhard Wischmeyer**

Date of Public Defence: …………………………………….…………

Date of Receipt of Certificates: ……………………………………………

Table of Contents

Abbreviations

A

AAC · Axo-axonic cell
ABC · Avidin-Biotin-Complex
ADHD · Attention deficit
    hyperactivity disorder
asf · Area sampling fraction

B

BDNF · Brain-derived
    neurotrophic factor

C

CA · Cornu ammonis
CB · Calbindin D28K
CCK · Cholecystokinin
CDH13 · Cadherin-13
cDNA · Complementary
    Deoxyribonucleic Acid
CR · Calretinin

D

DAB · 3,3' diaminobenzidine
    tetrahydrochloride
DG · Dentate gyrus
DNA · Deoxyribonucleic acid
DSM-5 · 5th edition of
    Diagnostic and Statistical
    Manual of Mental Disorders

E

EC · Entorhinal cortex
ER · Endoplasmic reticulum

F

FISH · Fluorescent in-situ-
    hybridization

G

GABA · γ-aminobutyric acid
GAD · Glutamate
    decarboxylase
Gad1 · Glutamate
    decarboxylase 1
GPI ·
    Glycosylphosphatidylinositol
GSK3ß · glycogen synthase
    kinase 3ß
GWAS · Genome-wide
    association studies

H

H_2O_2 · Hydrogen peroxide
HIER · Heat-induced epitope
    retrieval
HRP · Horseradish peroxidase

I

ISH · In-situ-hybridization

L

LTP · long-term potentiation

M

MLV · Murine leukemia virus
mRNA · Messenger RNA

N

nNOS · Nitric oxide synthase
NPY · Neuropeptide Y

O

OL-M · Oriens lacunosum-
    moleculare

P

PCR · Polymerase chain
    reaction
PFC · prefrontal cortex
PV · Parvalbumin

Q

qRT-PCR · Quantitative real-
    time polymerase chain
    reaction

R

REM · Rapid-eye-movement
RNA · Ribonucleic acid
ROCK · RhoA/Rho-kinase
RT · Reverse transcriptase
RTK · receptor tyrosine kinase

S

SL · Stratum lucidum
SLM · Stratum lacunosum-
    moleculare
SNP · Single Nucleotide
    Polymorphisms
SO · Stratum oriens
SOM · Somatostatin
SP · Stratum pyramidale
SR · Stratum radiatum
ssf · Section sampling fraction

T

TrkB · Tropomyosin-related
    kinase B

V

VIP · Vasointestinal peptide

Summary

Cadherin-13 (CDH13) is an atypical member of the cadherin superfamily, a group of membrane proteins mediating calcium-dependent cellular adhesion. Although CDH13 shows the classical extracellular cadherin structure, the typical transmembrane and cytoplasmic domains are absent. Instead, CDH13 is attached to the cell membrane via a glycosylphosphatidylinositol (GPI) anchor. These findings and many studies from different fields suggest that CDH13 also plays a role as a cellular receptor.

Interestingly, many genome-wide association studies (GWAS) have found *CDH13* as a risk gene for attention-deficit/hyperactivity disorder (ADHD) and other neurodevelopmental disorders.

In previous work from our research group, strong expression of *Cdh13* mRNA in interneurons of the hippocampal *stratum oriens* (SO) was detected. Therefore, double-immunofluorescence studies were used to evaluate the degree of co-expression of CDH13 with seven markers of GABAergic interneuron subtypes. For this purpose, murine brains were double stained against CDH13 and the respective marker and the degree of colocalization in the SO of the hippocampus was assessed.

Based on the result of this immunofluorescence study, quantitative differences in interneuron subtypes of the SO between *Cdh13* knockout (ko), heterozygote (het) and wildtype (wt) mice were investigated in this dissertation using stereological methods. In addition, genotype-dependent differences in the expression of genes involved in GABAergic and glutamatergic neurotransmission were analyzed by quantitative real-time PCR (qRT-PCR). Primers targeting different GABA receptor subunits, vesicular GABA and glutamate transporter, GABA synthesizing enzymes and their interaction partners were used for this purpose.

The results of the stereological quantification of the interneuron subtypes show no significant differences in cell number, cell density or volume of the SO between *Cdh13* ko, het and wt mice. On the other hand, qRT-PCR results indicate significant differences in the expression of tropomyosin-related kinase B gene (*TrkB*), which encodes the receptor of brain-derived neurotrophic factor (BDNF), a regulator of GABAergic neurons. This finding supports a role for CDH13 in the regulation of BDNF signaling in the hippocampus.

Zusammenfassung

Cadherine sind eine große Gruppe von calciumabhängigen Typ-1 Transmembranproteinen, die an der Ausbildung von Zell-Zell-Kontakten beteiligt sind. Cadherin-13 (CDH13) ist ein atypisches Mitglied dieser Proteinfamilie. Obwohl es die gleiche extrazelluläre Struktur wie klassische Cadherine besitzt, fehlen sowohl die cytoplasmatische als auch die Transmembrandomäne. Stattdessen ist CDH13 über einen GPI-Anker an der zellulären Plasmamembran befestigt. Diese Ergebnisse und viele andere Studien aus unterschiedlichen Bereichen lassen vermuten, dass CDH13 auch als zellulärer Rezeptor wirkt. Interessanterweise ergaben verschiedene genomweite Assoziationsstudien, dass *CDH13* ein vielversprechendes Kandidatengen für das Auftreten von Aufmerksamkeitsdefizit-/Hyperaktivitätsstörung (ADHS) und anderen Störungen der neuronalen Entwicklung ist.

In früheren Studien unserer Arbeitsgruppe wurde eine starke Expression von *Cd13* mRNA in Interneuronen des *stratum oriens* (SO) des Hippocampus festgestellt. Daher wurde mit Hilfe von Immunfluoreszenz der Grad der Koexpression von CDH13 mit 7 verschiedenen Markern von Subtypen GABAerger Interneuronen ermittelt. Zu diesem Zweck wurden Doppelfärbungen gegen CDH13 und den jeweiligen Marker durchgeführt und anschließend der Grad der Kolokalisation im SO des Hippocampus berechnet.

Ausgehend von diesen Ergebnissen wurden in dieser Dissertation quantitative Unterschiede zwischen verschiedenen Subtypen von Interneuronen in *Cdh13* knockout (ko), heterozygoten (het) und Wildtyp (wt)-Mäusen mit Hilfe von stereologischen Methoden ermittelt. Darüber hinaus wurden genotypabhängige Unterschiede in der GABAergen und glutamatergen Neurotransmission mit quantitativer Echtzeit-PCR (qRT-PCR) evaluiert. Hierzu wurden Primer eingesetzt, die sowohl auf Untereinheiten des GABA Rezeptors, GABA-synthetisierende Enzyme als auch auf GABA- und Glutamat-Transporter innerhalb synaptischer Vesikel abzielen. In der stereologischen Quantifizierung der Interneuron-Subtypen wurden keine signifikanten Unterschiede bezüglich der Zellzahl, der Zelldichte oder des Volumens des SO zwischen den verschieden Genotypen gefunden. Im Gegensatz dazu zeigten sich in der qRT-PCR signifikante Unterschiede in der Expression von tropomyosin-related kinase B (*TrkB*), einem Gen, das für den Rezeptor des brain-derived neurotrophic factor (BDNF) kodiert. Bei diesem handelt es sich um einen Regulator von GABAergen Neuronen. Diese Ergebnisse bekräftigen, dass CDH13 an der Regulation des BDNF-Signalwegs im Hippocampus teilnimmt.

1. Introduction

1.1 Attention deficit hyperactivity disorder (ADHD) and comorbid disorders

The 5th edition of *Diagnostic and Statistical Manual of Mental Disorders* (DSM-5) classifies ADHD as a neurodevelopmental disorder with the cardinal signs of inattention and hyperactivity/impulsivity, present for at least six months (American Psychiatric Association 2013).

These symptoms must be a significant limitation of the patient's functioning or development, play a role particularly as negative influence on social or academic activities, and be present in different settings. To fulfill the diagnosis of ADHD, at least 6 out of 9 criteria from inattention or hyperactivity/impulsivity symptoms must be met. This results in either a combined presentation of ADHD (criteria from both the inattention and hyperactivity/impulsivity group were diagnosed) or a predominantly form in which just criteria from one group are present.

The DSM-5 states a worldwide prevalence of about 5% in children and about 2.5% in adults. Males are affected up to 4 times more often by ADHD than females (Ford, Goodman et al. 2003). Furthermore significant variances in prevalence among different ethnic origins have been reported (Cuffe, Moore et al. 2005). It remains unclear if these may be caused by cultural variations regarding the interpretation of children's behavior (American Psychiatric Association 2013) or methodical artifacts (Williamson and Johnston 2015).

Contrary to widespread belief, there is no evidence of an increasing ADHD prevalence rate in the last decades. Large meta-analyses showed that different prevalence rates are rather based on improved diagnosis criteria, methodological differences of the studies or increased impairment (Polanczyk, Willcutt et al. 2014, Banaschewski, Becker et al. 2017).

The rate of treatment and diagnosis however grew constantly. While 0.9% of children in the US received ADHD treatment in 1987, the number increased to 3.4% in 1997 (Olfson, Gameroff et al. 2003). For a long time it has been assumed that ADHD has to been seen as a disorder of childhood that does not persist into higher age groups. This assumption was challenged by several follow-up studies of ADHD patients (Franke, Faraone et al. 2012). A large meta-analysis showed that about 15% of follow-up patients met full ADHD criteria at the age of 25 and about 65% met partial remission criteria, thus fewer symptoms with still existing impairment (Faraone, Biederman et al. 2006). As mentioned before, more recent

epidemiological studies and meta-analyses estimate the prevalence in adults at 2.5%, leaving no doubt that ADHD persists into adulthood at a high rate (Simon, Czobor et al. 2009).

Both ADHD symptoms and the resulting impairment show great variability among different social, academic or occupational demands (Banaschewski, Becker et al. 2017). Hyperactivity is most prominent in children up to the age of six, while inattention is more often observed at primary school age. In adulthood, impulsivity and restlessness might be brought to the fore (American Psychiatric Association 2013). Furthermore, there are several common problems associated with ADHD, such as non-compliant behavior, sleep disturbance or aggression (National Collaborating Centre for Mental Health 2009). ADHD affects academic and occupational performance as well as social interaction. ADHD patients tend to have lower educational levels and higher unemployment rates (Lara, Fayyad et al. 2009). Their relationships with family and peers are often characterized by disharmony or negative interactions on the one side and rejection or neglect on the other (American Psychiatric Association 2013).

In addition, comorbid psychiatric disorders are a common feature in ADHD patients. In a large Danish sample, 52% of the patients had at least one comorbid psychiatric disorder, while 26% had two or more (Jensen and Steinhausen 2015). Disorders most often co-occurring are oppositional defiant disorder, conduct disorder, anxiety disorder, autism spectrum disorders as well as intellectual disability and learning disorders (Wells, Chi et al. 2006, Jensen and Steinhausen 2015).

1.2 Molecular genetics of ADHD

ADHD is a very heterogeneous disorder. Although the etiology of ADHD is subject of intensive research, it is not yet completely understood (Bonvicini, Faraone et al. 2016).

Most studies from the last decades indicate a strong genetic component. Biological children from ADHD families have an increased risk to develop the disorder, while adopted children shared the same risk with the control group (Sprich, Biederman et al. 2000). This assumption is backed by several twin studies that estimate a heritability of about 75% by comparing identical and fraternal twins (Faraone, Perlis et al. 2005). Further approaches to unveil the complex genetic structure of ADHD are linkage scans. They are performed to identify genetic loci potentially involved in the pathogenesis. In the last years, several linkage scans identified large numbers of susceptibility loci, either in sibling-pair samples (e.g. Faraone, Doyle et al. 2008) or in large pedigrees (e.g. Romanos, Freitag et al. 2008).

A meta-analysis including seven of those studies found genome-wide significant linkage on chromosome 16 bin 4 (16q23.1-qter), respectively 64 – 83 Mb on closer analysis (Zhou, Dempfle et al. 2008). The section contains more than 200 genes, including the cell-adhesion molecule Cadherin-13 (*CDH13*). Furthermore, nine other genomic loci with either nominal or suggestive evidence of linkage were described. In complex traits, however, linkage analysis rather serves as a screening tool as it primarily identifies large loci with moderate effects (Franke, Faraone et al. 2012, Li, Chang et al. 2014). They are therefore better suited for the investigation of monogenic diseases (Franke, Neale et al. 2009).

On the contrary, genome-wide association studies (GWAS) are the method of choice to detect genes with modest effect (Risch and Merikangas 1996). Instead of actual genes, hundred thousands of defined *Single Nucleotide Polymorphisms* (SNP) markers are used to identify association with complex phenotypes. GWAS do not require prior selection of candidate genes and are therefore unbiased and hypothesis-free regarding the genetics of a trait (Franke, Neale et al. 2009, Stranger, Stahl et al. 2011). However, large sample sizes are needed, as neurodevelopmental disorders, such as ADHD, tend to have risk genes with very small effect sizes (Lesch, Timmesfeld et al. 2008).

In the last decade, numerous GWAS on ADHD have been carried out. The NHGRI-EBI Catalog of published genome-wide association studies lists 33 GWAS covering either ADHD or an associated phenotype (MacArthur, Bowler et al. 2017). One of the first was conducted in 2008, when Lesch, Timmesfeld et al. found associations with several SNPs in pooled deoxyribonucleic acid (DNA). Although not reaching the genome-wide threshold, the study unveiled several new candidate genes and emphasized the role of *CDH13* as crucial factor in the pathogenesis of ADHD. This assumption is supported by the observation that association with *CDH13* was found in 3 GWAS with otherwise very limited overlap (Franke, Neale et al. 2009).

To increase the statistical power of the GWAS, Neale, Medland et al. (2010) carried out a meta-analysis of four major studies but did not reach genome-wide significance either. Therefore, it has been suggested to further enlarge sample sizes and enhance international collaboration (Li, Chang et al. 2014). Interestingly, a most recent study reported formal genome-wide significance for executive inhibition in ADHD children (Yang, Chang et al. 2017). The authors hypothesize that different endophenotypes of complex traits may have different etiologies and therefore should be studied separately.

In contrast to the GWAS approach that uses DNA markers throughout the whole genome, candidate gene studies are a more powerful tool for direct gene discovery (Zhu and Zhao

2007). The investigator selects genes that are potentially relevant for the etiology, based for example on neurobiological findings, logical considerations or data from related disorders (Kwon and Goate 2000). Allele frequencies are either compared between an experimental group with ADHD patients and a control group, or between transmitting parents and children (Faraone, Perlis et al. 2005). It has to be pointed out, that the method is very limited if the etiology of a trait is still unclear, as it is dependent on correct presumptions (Zhu and Zhao 2007).

Most candidate studies focus on neurotransmission systems, particularly on dopaminergic, but also on noradrenergic and serotonergic systems (Banaschewski, Becker et al. 2010). The database ADHD gene lists 24 candidate genes with dopamine transporter (*SLC6A3*) and receptor (*DRD4*, *DRD5*) genes reaching the highest counts on studies conducted (Zhang, Chang et al. 2012). This is not surprising as the gene products are targets of methylphenidate, the most common anti-ADHD drug. The results however, remain inconsistent with both positive and negative findings. Possible ethnicity effects and variable risks for functional variants have been discussed, leaving need for further research and larger samples (Banaschewski, Becker et al. 2010).

In summary, there is strong evidence that ADHD has a large genetic component with several different genes involved. It can be assumed that, among others, *CDH13* plays a substantial role in the etiology.

1.3 Hippocampal neuroanatomy and function with particular focus on hippocampal interneurons

The hippocampus forms an integral part of the limbic system and is located in the medial temporal lobe of the brain. The hippocampus proper consists of the *cornu ammonis* (CA). Together with the *dentate gyrus* (DG), *subiculum, parasubiculum* and *entorhinal cortex* (EC), it forms a functional brain system called the hippocampal formation (Andersen 2007). The hippocampus proper itself can be further divided into subfields CA1, CA2 and CA3 in proportion to the DG (Lorente de Nó 1934). Several intrinsic pathways connect the different structures of the hippocampal formation with each other (Figure 1), of which the trisynaptic circuit might be the most prominent example. The term describes the excitatory loop between the EC → DG (synapse I), DG → CA3 (synapse II) and CA3 → CA1 (synapse III) before returning to the EC (Andersen, Bliss et al. 1971, Andersen 2007).
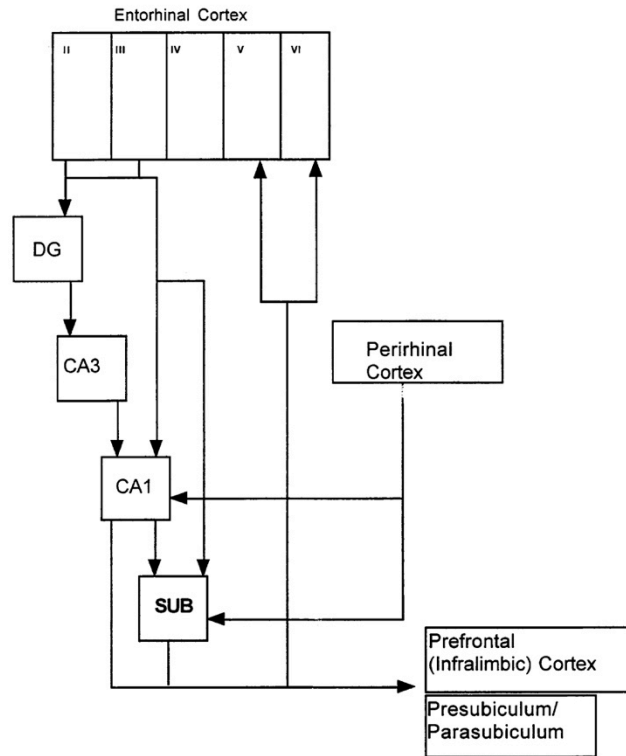
Figure 1: Overview of the intrinsic connection within the hippocampal formation. Reproduced from: O'Mara, Commins et al. (2001) with permission from Elsevier.

Unlike the *neocortex*, which forms the largest part of the brain and typically consists of six horizontal cell layers, the hippocampus is part of the *allocortex* showing a different organization (Mendoza and Foundas 2008). The hippocampus proper has five neuronal layers (Figure 2):

The *stratum pyramidale* (SP) contains most of the cell bodies, mainly pyramidal excitatory cells, which form the principal neuronal cells of the hippocampus. They usually have large dendritic trees that reach both the apical and basal sites, although variations in between neurons of different subfields can be observed (Andersen 2007).

The thin *stratum lucidum* (SL) is located above the SP only in CA3, whereas it does not exist in CA1 or CA2. It contains mossy fibers, axons from dentate granule cells that project exclusively into the CA3 (Andersen 2007). The *stratum radiatum* (SR) is located above the SL in CA3 and directly apical of the SP in CA1 and CA2, respectively. It accommodates the so called Schaffer collaterals, axons that project from CA3 to CA1 (Andersen 2007).

Afferent fibers from several regions terminate in the *stratum lacunosum-moleculare* (SLM), including the *entorhinal cortex* and the *thalamus* (Andersen 2007).

The *stratum oriens* (SO) is located below the SP and does not only contain basal dendrites from the pyramidal cells, but also the somata of different types of interneurons (Freund and Buzsaki 1996, Andersen 2007).
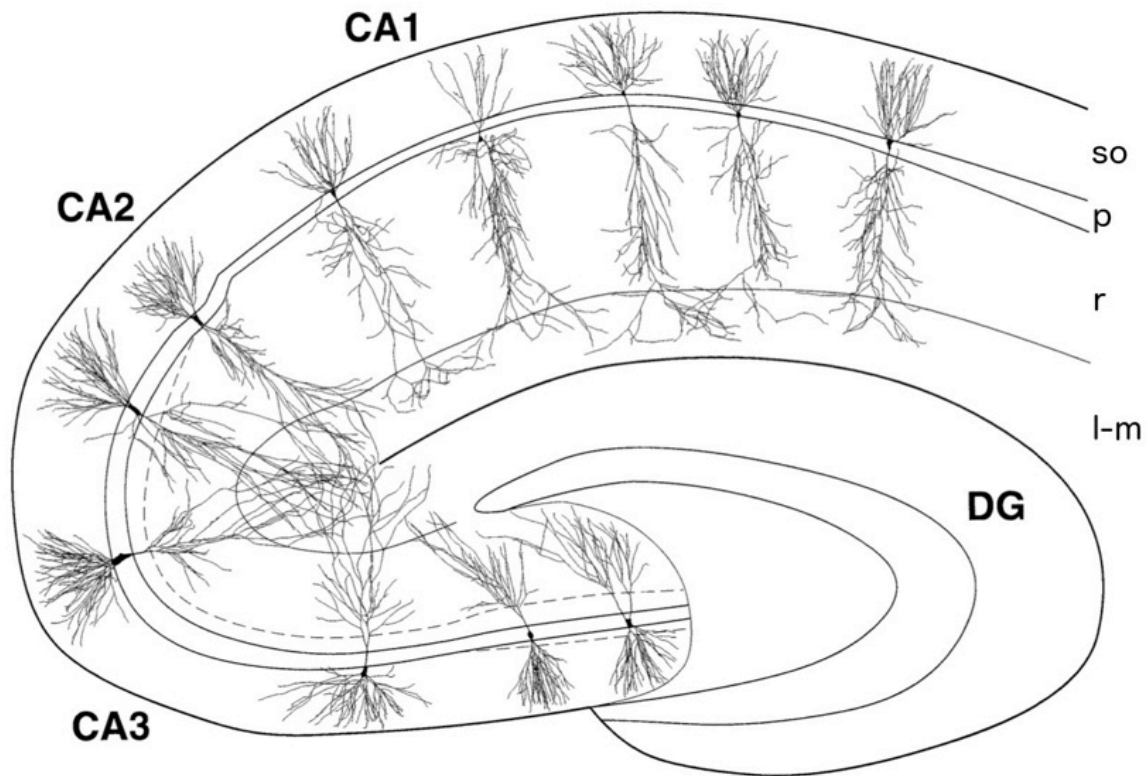

Figure 2: Schematic overview of the hippocampus including computer-generated pyramidal cell projections. The cell body is located in the stratum pyramidale. Dendrites reach both to the apical (stratum radiatum) and the basal side (stratum oriens). The dotted line in CA3 indicates the stratum lucidum. Abbreviations: CA1, cornu ammonis area 1; CA2, cornu ammonis area 2; CA3, cornu ammonis area 3; DG, dentate gyrus; LM, stratum lacunosum-moleculare; r, stratum radiatum; p, stratum pyramidale; so, stratum oriens. Reproduced from: Ishizuka, Cowan et al. (1995) with permission from John Wiley and Sons.

In this thesis, the term interneurons refers to cells of the cerebral cortex that use γ-aminobutyric acid (GABA) as neurotransmitter according to the Petilla terminology (Ascoli, Alonso-Nanclares et al. 2008). Inhibitory interneurons in the hippocampus show great diversity. Before being integrated into neural circuits, different subtype specifications are determined, which vary both in their morphology and physiology (Figure 3) (Batista-Brito, Machold et al. 2008, Ramamoorthi and Lin 2011, Rivero, Selten et al. 2015).

Unlike the principal pyramidal cells of the hippocampus, interneurons have different postsynaptic domains and are therefore able to perform different tasks (Freund and Buzsaki 1996, Leao, Mikulovic et al. 2012). Despite their small number (interneurons account for only

11

7% of all hippocampal neurons), they play a crucial role in the coordination of cortical processing by pacing and synchronizing excitatory neuron populations (Aika, Ren et al. 1994, Klausberger and Somogyi 2008, Tricoire, Pelkey et al. 2011). Prominent examples are theta oscillations (4-10 Hz), which appear not only during rapid-eye-movement (REM) sleep, but also during memory tasks and spatial navigation (Klausberger and Somogyi 2008).

Low activity and the disruption of inhibitory circuits can lead to hyperexcitability and resulting pathologies (Marin 2012). Not only a link to epilepsy has been discussed, but also their role in the pathogenesis of developmental disorders such as autism or ADHD is subject of research (Galanopoulou 2010, Ramamoorthi and Lin 2011, Marin 2012).
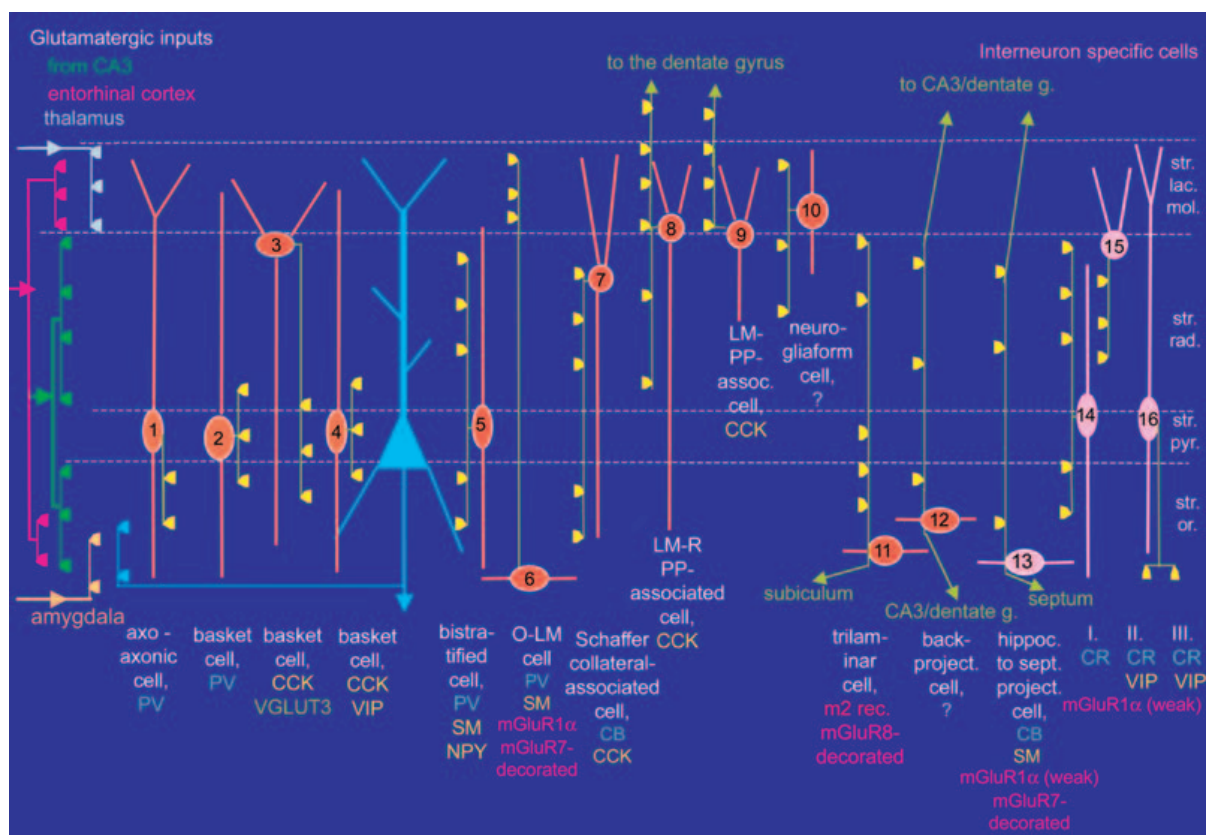

Figure 3: Different types of hippocampal interneurons in the CA1 area. Green lines: axons. Yellow triangles: termination zone of GABAergic synapses. Orange somata and dendrites: interneurons innervating pyramidal cells. Pink somata and dendrites: interneurons mainly innervating other interneurons. A list of expressed chemical markers is included under the neuron's proposed names. Abbreviations: CB, calbindin; CR, calretinin; LM-PP, lacunosum-moleculare–perforant path; LM-R-PP; lacunosum-moleculare–radiatum–perforant path; m2, muscarinic receptor type 2; NPY, neuropeptide tyrosine; PV, parvalbumin; SM, somatostatin; VGLUT3, vesicular glutamate transporter 3. Reproduced from: Somogyi and Klausberger (2005) with permission from John Wiley and Sons.

Since the first description of hippocampal neurons by Ramón y Cajal (1893), which only distinguished between "pyramidal" and "nonpyramidal" cells, it took more than 70 years until Colonnier (1965) emphasized the diversity of different interneurons (Freund and Buzsaki 1996). Ever since major efforts to characterize these cells have been made. Nowadays, the

type of pyramidal cell innervation is the most common standard to characterize hippocampal interneurons (Leao, Mikulovic et al. 2012). More than 21 different types of hippocampal interneurons have been reported (Klausberger and Somogyi 2008). In the following, only those that have been adequately investigated and relevant to this thesis will be discussed.

The pyramidal basket cells are a large and heterogeneous group with a variety of morphologies and locations (Andersen 2007). As common feature, they innervate the perisomatic regions directly, thus soma or proximal dendrites of principal cells (Freund and Buzsaki 1996). This special innervation pattern enables the basket cells to affect all inputs that the pyramidal cell receive (Müller and Remy 2014).

Axo-axonic cells (AAC) or chandelier cells were first described in the neocortex. In the hippocampus, they are located close to the pyramidal cells. The name derives from lines of axo-axonic synapses that they form exclusively with initial segments of pyramidal cell axons (Freund and Buzsaki 1996, Contreras 2004, Szabadics, Varga et al. 2006, Andersen 2007). Interestingly, alterations in this type of cells have been reported in patients with schizophrenia (Joseph N. Pierri, Adil S. Chaudry et al. 1999).

The cell bodies of the oriens lacunosum-moleculare cells (O-LM) are located in the SO, while their axons ascend directly to the SLM, where they form synapses with distal dendrites of principal cells, which also receive direct input from the entorhinal cortex (Freund and Buzsaki 1996, Andersen 2007, Leao, Mikulovic et al. 2012).

Another type of interneurons are bistratified cells. Their somata are mainly located in the SP and SO and their axons form a typical 2-layered pattern both in the SR and SO, giving those cells their name. The dendritic trees span through all layers, but do not reach the SLM. They receive excitatory inputs from Schaffer collaterals and commissural projections and are strictly regulated by inhibitory inputs from other local interneurons such as OLM. They constitute about 6% of all hippocampal interneurons (Freund and Buzsaki 1996, Andersen 2007, Klausberger 2009, Bezaire and Soltesz 2013, Müller and Remy 2014).

Trilaminar cells are a group of interneurons that was first described by Sik, Penttonen et al. (1995). Some authors further distinguish them into horizontal and radial trilaminar cells depending on their predominant orientation (Figure 3) (Freund and Buzsaki 1996). The name of the trilaminar cells derives from the observation that their axons innervate the three layers SO, SP and SR (Somogyi and Klausberger 2005). Furthermore, trilaminar cells have been shown to project to the *fimbria* of the *subiculum* (Sik, Penttonen et al. 1995). Unlike most other GABAergic interneurons, trilaminar cells are able to fire bursts with high frequency (Klausberger 2009).

Hippocampo-septal cells are a subtype which mainly innervates other hippocampal GABAergic interneurons that are located either in proximity to the soma in the SO or in remote areas connected to the hippocampal formation such as the septum (Gulyas, Hajos et al. 2003, Somogyi and Klausberger 2005).

Morphological and electrophysiological properties based on single-cell studies are not the only ways to characterize hippocampal cells. Nearly all interneurons can be immunolabeled with chemical markers, which have proven to be a very effective way to subdivide different interneuron populations. Typical markers include neuropeptides such as neuropeptide Y (NPY), somatostatin (SOM), cholecystokinin (CCK) and vasoactive intestinal protein (VIP) as well as calcium-binding proteins such as parvalbumin (PV), calretinin (CR) and calbindin D28K (CB) (Jinno and Kosaka 2006).

It must be emphasized that most chemical markers are expressed in more than one cell type and therefore cannot be seen as sole criterion for a definite determination of a neuron class (Figure 4) (Somogyi and Klausberger 2005). However, they represent the method of choice for quantitative evaluation of large cell numbers as performed in this thesis. Furthermore, they offer an opportunity to check the results of single-cell studies for consistency throughout large neuronal networks (Freund and Buzsaki 1996, Jinno and Kosaka 2006).
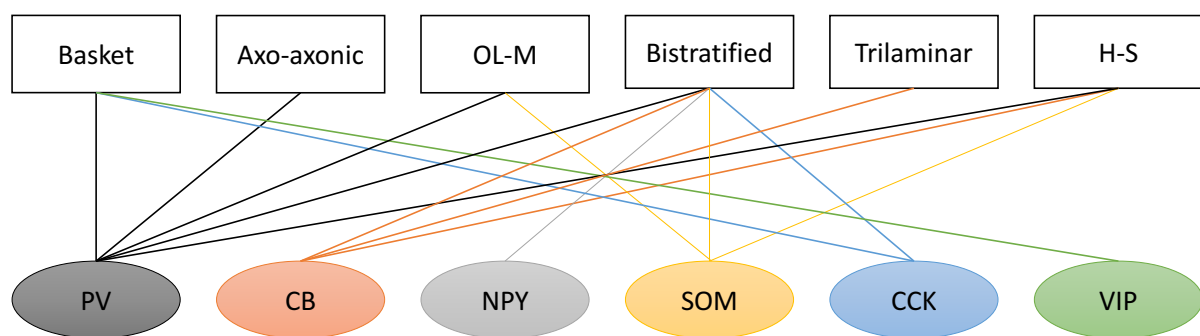

Figure 4: Different subpopulations of GABAergic interneurons, defined by their expression of chemical markers. Abbreviations: O- LM, oriens lacunosum-moleculare; H-S, hippocampo-septal projection cell; PV, parvalbumin; CB, calbindin D28K; NPY, neuropeptide Y; SOM, somatostatin; CCK, cholecystokinin; VIP, vasointestinal peptide. Adapted from: Jinno and Kosaka (2006).

Even though the other parts of the hippocampal formation are of minor importance in the context of this thesis, they shall be addressed briefly in the section below as they play a crucial role in hippocampal circuitry and function.

Unlike the remaining hippocampal formation, the ER has six layers that rather resemble those of the isocortex. While layer I is cell-poor and accommodates fibers, layers II and III are

populated by neurons that project to the DG, CA3, CA1 and the *subiculum* via the perforant path, a connectional route of afferent axons. The deep layers are separated from the superficial region by the cell-free *lamina dissecans* which forms layer IV. Layers V and VI, in turn, are rich in different classes of neurons that project to deep white matter and also form local circuits within the EC (Andersen 2007). The EC is considered to serve as the main junction for inputs that reach the hippocampal formation from all associated cortex regions (Figure 1) (Fyhn, Molden et al. 2004). Most input is provided by the perirhinal and parahippocampal cortices (Lavenex and Amaral 2000), which connect to the hippocampus mainly via the perforant path (Mendoza and Foundas 2008).

The DG is a U or V-shaped region with a simple cortical structure consisting of three layers: The granule cell layer contains almost exclusively granule cells, the principal cells of the DG, which send unmyelinated axons called mossy fibers to CA3. The molecular layer contains the afferent fibers from the perforant path. On the contrary, the polymorphic cell layer accommodates different types of cell populations, including interneurons and mossy cells that synapse prominently with mossy fibers in thorny excrescences on their way to CA3 (Amaral, Scharfman et al. 2007). As the DC receives extensive unidirectional input from the EC via the perforant path, it is seen as a "preprocessor" of sensory information, which subsequently reaches the hippocampus proper via the mossy fibers (Jonas and Lisman 2014).

The *subiculum* is located between CA1 and the ER and can be seen as outmost layer of the hippocampal formation (Mendoza and Foundas 2008, Ding 2013). It has three layers (molecular layer, pyramidal cell layer and polymorphic layer) and two different types of principal cells that can be distinguished (O'Mara, Commins et al. 2001). While these cells hardly differ in their morphology, they show disparities in both their physiology and connectivity (Andersen 2007). The *subiculum* mediates the major part of hippocampal output and can, to some extent, be regarded as counterpart of the EC (Mendoza and Foundas 2008). Via its reciprocal projections to the EC as well as direct connections to neocortex and *amgydala*, the *subiculum* is a key factor in the distribution of information processed in the hippocampus (Andersen 2007, Eller, Zarnadze et al. 2015).

The function of the hippocampus has been closely linked to memory for a long time. In the 1950s, the observation of patients with medial temporal lobe lesions who suffered from amnesia (Scoville and Milner 1957) marked a milestone in the investigation of the hippocampal region (Andersen 2007, Preilowski 2009). Ever since, major efforts were undertaken to unveil the functional role of the hippocampus.

It is now understood that the hippocampus plays a crucial role in the formation of different types of memories. It has to be acknowledged, however, that the function of the hippocampal formation cannot be seen in isolation, as other brain areas and networks are largely involved as well (Andersen 2007). Cohen and Squire (1980) showed that amnesia patients with lesions of the hippocampal formation lacked declarative memory (facts and events), while their non-declarative memories (motor and cognitive skills) remained intact (Squire 2004, Squire, Stark et al. 2004, Andersen 2007). Interestingly, vocabulary, short-term memory as well as memories which were acquired long before the lesion are also preserved in these patients (Bird and Burgess 2008). In the sequel, several theories have been postulated which all emphasize the role of the hippocampus in the mediation of episodic memory but provide different explanatory approaches (Nadel and Moscovitch 1997, Squire, Stark et al. 2004, Bird and Burgess 2008).

The function of the hippocampus is not limited to memory, though. O'Keefe and Dostrovsky (1971) described "place-cells", hippocampal neurons whose activity is dependent of the animal's position within a specific environment. They therefore concluded that the hippocampus must be involved in spatial navigation (Schiller, Eichenbaum et al. 2015). Because of its simplicity, elegance and self-evidence, the theory was highly successful and marked an evolution beyond the field of hippocampus research (Stella, Cerasti et al. 2012). The assumption that the hippocampus plays an important role in navigation is backed by lesion studies, in which impaired animals performed worse in the Morris water maze (Morris 1984), a task that is specific for spatial ability (Stella, Cerasti et al. 2012). The hippocampus has also been linked to fear learning and expression. Together with the amygdala and the medial prefrontal cortex, the hippocampus is believed to form a neural network processing fear through long-term potentiation (LTP) (Toyoda, Li et al. 2011, Tovote, Fadok et al. 2015).

1.4 GABAergic neurotransmission

GABA is the main inhibitory neurotransmitter in the CNS and can be found in 30% of all synapses (Sieghart and Sperk 2002). It is also of major clinical importance. Alterations in brain GABA levels have been found in several psychiatric and neurological disorders, including schizophrenia, autism spectrum disorder, major depressive disorder, insomnia and epilepsy (Olsen, DeLorey et al. 1999, Möhler 2006, Schür, Draisma et al. 2016). Several drugs modulate GABAergic neurotransmission including benzodiazepines, anesthetics and anticonvulsants (Sieghart and Sperk 2002).

GABA is produced by alpha-decarboxylation of glutamate, which is catalyzed by the glutamate decarboxylase (GAD) (Figure 5). GAD activity, and thus GABA concentration in the brain, is regulated by cofactor-dependent interconversion between an active and inactive (apo) form of the enzyme (Martin and Rimvall 1993, Petroff 2002).
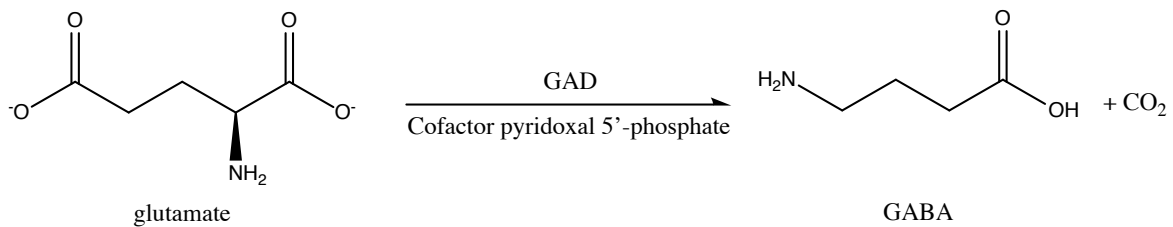

Figure 5: Synthesis of GABA from glutamate.

In mammals, several isoforms and splicing variants of GAD have been described. Only two of them are believed to have catalytic activity: GAD65 and GAD67 are encoded by the two independently regulated genes *GAD2* and *GAD1* and seem to have different functions and subcellular locations. GAD65 appears to provide GABA for synaptic vesicles. GAD67 synthesizes GABA for cytoplasmic use within GABAergic neurons (Soghomonian and Martin 1998).

There are to two types of transmembrane receptors to be that mediate a biphasic response to the release of GABA (Couve, Moss et al. 2000). GABA A receptors are ligand-gated chloride ion channels that facilitate immediate inhibitory actions in the brain (Jacob, Moss et al. 2008). They consist of 5 different subunits in varying composition (Figure 6). Until now, seven classes of subunits with different numbers of members have been identified: α (1–6), β (1–3), γ (1–3), δ, ε (1–3), θ and π (Sieghart and Sperk 2002, Jacob, Moss et al. 2008). Most receptors contain a combination of α, β and γ subunits (only the latter can be replaced by δ, ε and π). This results in a great number of structural variants, which can be even increased by alternative splicing (Jacob, Moss et al. 2008).
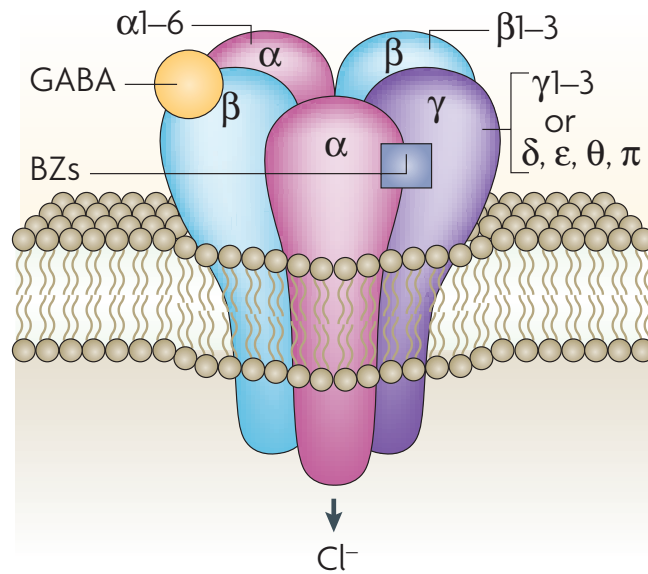
Figure 6: The GABA A receptor is a heteropentameric ion channel that consists of 5 subunits. GABA binds between the alpha and the beta subunit and triggers a chloride flow into the cell. BZs = benzodiazepine binding side. Reproduced from: Jacob, Moss et al. (2008) with permission from Springer Nature.

GABA B receptors are metabotropic receptors that mediate the slower response to the neurotransmitter. They belong to the group of G protein–coupled receptors, which activate a signaling cascade upon ligand binding (Couve, Moss et al. 2000). GABA B receptors are also located in extrasynaptic regions where they have been linked to a wide range of neuronal processes, including neuronal migration and plasticity (Couve, Moss et al. 2000, Bettler, Kaupmann et al. 2004).

Several receptor-associated proteins were found to interact with GABA receptors. A prominent example is gephyrin, a scaffold protein in the postsynaptic membrane of inhibitory synapses anchored to certain receptor subtypes and the cytoskeleton. Regulated by multiple pathways, gephyrin can modify the clustering of GABA and glycine receptors and thus its composition and stability (Jacob, Moss et al. 2008, Tyagarajan and Fritschy 2014).

1.5 The Cadherin superfamily

Cadherins are a superfamily of calcium-dependent cell-cell adhesion molecules, first discovered in morula compaction in the early 1980s. They can be divided into subfamilies of classical or type I cadherins, atypical or type II cadherins, protocadherins, desmosomal cadherins and Flamingo cadherins. In addition there are several unconventional cadherins that

cannot be grouped, including CDH13 (Nollet, Kools et al. 2000). While all of the numerous family members have 5 to 34 calcium-binding cadherin repeats on the extracellular side as common feature, the remaining structure shows great variability, including the cytoplasmic region. Type I and type II cadherins interact with actin filaments of the cytoskeleton via a β-catenin and α-catenin complex. Others such as desmosomal cadherins are connected to intermediate filaments via plakoglobin or plakophilin with desmoplakin (Angst, Marcozzi et al. 2001, Resink, Philippova et al. 2009).

Classical cadherins are best known as cellular adhesion molecules. Particularly as transmembrane section of the adherens junction, they play a significant role in providing mechanical adhesion in epithelial tissue (E-cadherin and P-cadherin), endothelial tissue (VE-cadherin) as well as in neural tissue (N-cadherin) (Wheelock and Johnson 2003, Derycke and Bracke 2004). The function of cadherins is not limited to cell adhesion. Furthermore, they affect many signaling pathways, mainly during development and morphogenesis controlling cell sorting, planar cell polarity and proliferation in almost every tissue (Halbleib and Nelson 2006, van Roy and Berx 2008). This includes neuronal recognition, axon guidance and synapse formation in the central nervous system (Takeichi 2007).

Cadherins also play a crucial role in pathological processes, particularly in cancer. E-Cadherin is considered a tumor suppressor in the tumor genesis and metastasis of ductal breast cancer (Christofori and Semb 1999, Berx and Van Roy 2001).

1.6 Cadherin-13

CDH13 (also "truncated" or T-cadherin) is an unconventional cadherin that was first cloned in the 1990s from chick embryo (Ranscht and Dours-Zimmermann 1991).

The *CDH13* gene is located on human chromosome 16 (bin 4, 82.63 – 83.8 Mb) and consists of 1,169,627 base pairs containing 14 exons. It codes for a preprotein of 713 amino acids with five extracellular cadherin repeats (Lee 1996, Philippova, Joshi et al. 2009). These, however, show several structural differences compared to classical cadherins that also express five cadherin repeats. This includes the lack of many amino acids involved in mechanical adhesion in classical cadherins (Dames, Bang et al. 2008). As a consequence, CDH13 is not able to establish a cell-cell adhesion via swapping strands on the N-terminal repeat and therefore shows lower adhesiveness than classical cadherins (Ciatto, Bahna et al. 2010). CDH13 also

differs in other structural findings (Figure 7). Not only does it lack the cytoplasmic region but also it is connected to the plasma membrane through a glycosylphosphatidylinositol (GPI) anchor (Ranscht and Dours-Zimmermann 1991).
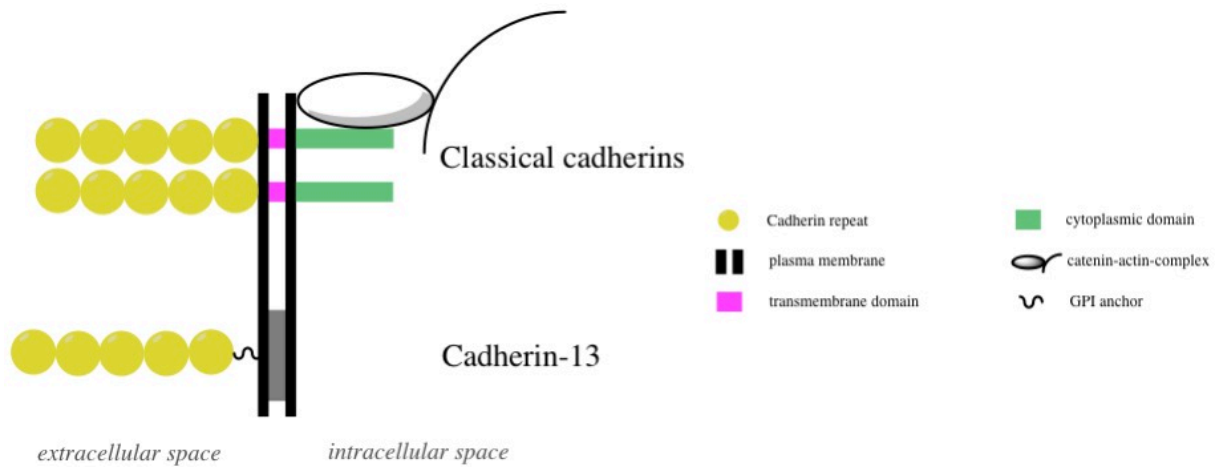

Figure 7: Schematic overview of the differences in the characteristics of classical cadherins and CDH13. In the classical cadherins, the extracellular cadherin repeats and the intracellular cytoplasmic part are connected via a transmembrane domain. CDH13 lacks an intracellular part and is attached to the plasma membrane via a GPI anchor. Adapted from: Angst, Marcozzi et al. (2001).

The unique structure and the low adhesion activity suggest that CDH13 holds a special role within the cadherin superfamily. CDH13 is widely distributed among different tissues. It shows high expression in the cardiovascular system, particularly in migrating cells in blood vessels (Philippova, Ivanov et al. 2003). Interestingly, the expression level is increased in atherosclerotic endothelial lesions in vivo as well as in proliferating and apoptotic cells in vitro (Philippova, Joshi et al. 2009).

Furthermore, CDH13 is highly expressed in the nervous system, where it was first described. Takeuchi, Misaki et al. (2000) reported the expression pattern in the human brain, showing CDH13 expression in the cerebral cortex, thalamus, midbrain and medulla oblongata, with particularly high expression in the olivary nuclei. In addition, they also found out that the expression of CDH13 in the adult brain is higher than in the developing brain. Previous work from our laboratory on the murine brain showed that *Cdh13* Ribonucleic acid (RNA) is expressed in neocortex, anterior cingulate cortex, hippocampus, thalamus, locus coeruleus and raphe nuclei, while CDH13 protein was found in the hippocampus and cortical areas (Rivero, Sich et al. 2013). Other organs, such as the liver, show either no CDH13 expression or its role remains unclear (Philippova, Joshi et al. 2009).

Early studies proposed CDH13 as negative regulator in neurite outgrowth (Rauscht and Dours-Zimmermann 1991, Fredette and Ranscht 1994, Fredette, Miller et al. 1996). Ever since, several different interaction partners and signaling effectors of CDH13 have been identified, which suggest a more complex function of the protein.

In endothelial cells, CDH13 was found to regulate the actin cytoskeleton via Rho-family GTPases, which in turn are the key regulators of pathways involved in cell migration (Raftopoulou and Hall 2004, Philippova, Ivanov et al. 2005). Through the RhoA/Rho-kinase (ROCK) pathway, CDH13 can modulate cell contraction and also control stress fiber assembly and the inhibition of spreading, while the formation of lamellipodia at the leading edges of polarized cells is Rac pathway dependent (Philippova, Ivanov et al. 2005).

Furthermore, CDH13 has been shown to influence the PI3K/Akt/GSK3 pathway in endothelial cells (Joshi, Ivanov et al. 2007). This pathway and its downstream effectors regulate cell growth, survival and metabolism and are particularly known for their key role in cancer pathogenesis (Hassan, Akcakanat et al. 2013). In the brain, the pathway is involved in neuronal survival. Downstream of Akt, several molecules including glycogen synthase kinase 3ß (GSK3ß) and ß-catenin were shown to control neurite outgrowth, synaptogenesis and synaptic transmission (Read and Gorman 2009, Rivero, Sich et al. 2013). Interestingly, Akt and GSK3 in the brain are also highly regulated by the monoamines dopamine (DA) and serotonin (5-HT), which in turn are a main target of psychiatric medication (Beaulieu 2012). Furthermore, atypical antipsychotics such as risperidone lead to a dose-dependent increase in the brain levels of active GSK3 (Li, Rosborough et al. 2007). Therefore it has been suggested that this pathway may contribute to the etiology of neurodevelopmental disorders (Emamian, Hall et al. 2004, Li, Rosborough et al. 2007).

The PI3K/Akt/GSK3 pathway can be activated by several receptors, including brain-derived neurotrophic factor (BDNF) receptor, tropomyosin-related kinase B (TrkB) (Rivero, Sich et al. 2013). TrkB plays an important role in GABAergic interneuron development, maturation and survival, particularly in the hippocampus (Alcantara, Frisen et al. 1997, Huang, Kirkwood et al. 1999, Yamada, Nakanishi et al. 2002). BDNF modulates trafficking of the GABA transporter GAT-1 and enhances GABA reuptake (Vaz, Jorgensen et al. 2011). Additionally, CDH13 is directly involved in the regulation of inhibitory synapses: Paradis, Harrar et al. (2007), showed that CDH13 acts as a promoter of synapse formation in murine hippocampal GABAergic and glutamatergic interneurons.

Taken together, these findings make it likely that CDH13 and its downstream effectors are involved both in neuron guidance and in regulation of synaptic plasticity in the central nervous system.

1.7 Distribution of CDH13 in different interneuron populations of the murine hippocampus

In previous work from our laboratory, *Cdh13* mRNA was detected in the murine hippocampal formation using *in situ* hybridization (ISH). Highest cellular expression was found in the SO of the hippocampal CA (Rivero, Selten et al. 2015). These findings are consistent with immunohistochemical analysis of CDH13 protein, which found the same pattern. The distinct expression of CDH13 in scattered cell bodies of the SO suggests that these cells might be interneurons, as their presence in the SO is well documented (Jinno and Kosaka 2006, Andersen 2007). For confirmation, a two-color *fluorescent in situ* hybridization (FISH) with staining against *Cdh13* and Glutamate decarboxylase 1 (*Gad1*) mRNA was performed. It revealed that most of the *Cdh13* positive cells were GABAergic interneurons (GAD is the synthesizing enzyme of GABA) (Figure 8).
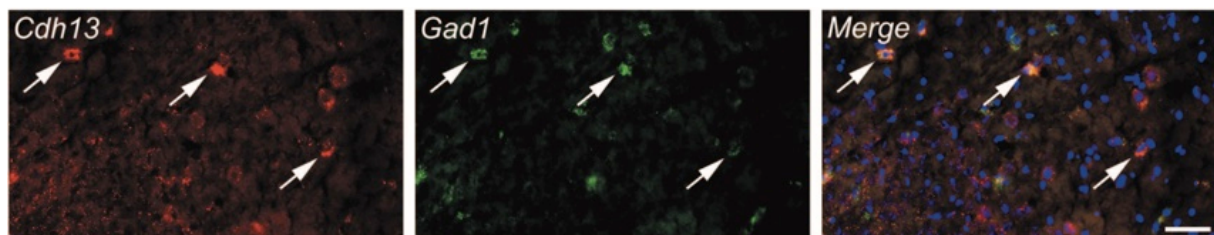

Figure 8: *Cdh13* positive cells in the hippocampus show high co-expression with *Gad1* in the double-FISH. Scale bars 50 μm. Reproduced from: Rivero, Selten et al. (2015), licensed under <u>CC BY 4.0</u>.

As mentioned before, the detection of chemical markers is the most effective method to characterize large interneuron populations. It allows a fast and effective classification into different groups, although overlapping is a limitation (Figure 4) (Somogyi and Klausberger 2005, Jinno and Kosaka 2006). To this end, quantification of the degree of coexpression between several of those chemical markers (calcium-binding proteins, neuropeptides and enzymes) and CDH13 was carried out. Different levels of coexpression among different markers resulted. The highest levels of coexpression in CDH13 positive cells were found with somatostatin (SOM) and parvalbumin (PV), the lowest with neuronal nitric oxide synthase (nNOS) and calretinin (CR) (Figure 9 A). Concurrent analysis of the rate of CDH13 expression

in each marker cell population was performed, with CDH13 most often found in PV-positive and SOM-positive cells. nNOS positive cells showed lowest CDH13 expression (Figure 9 B).
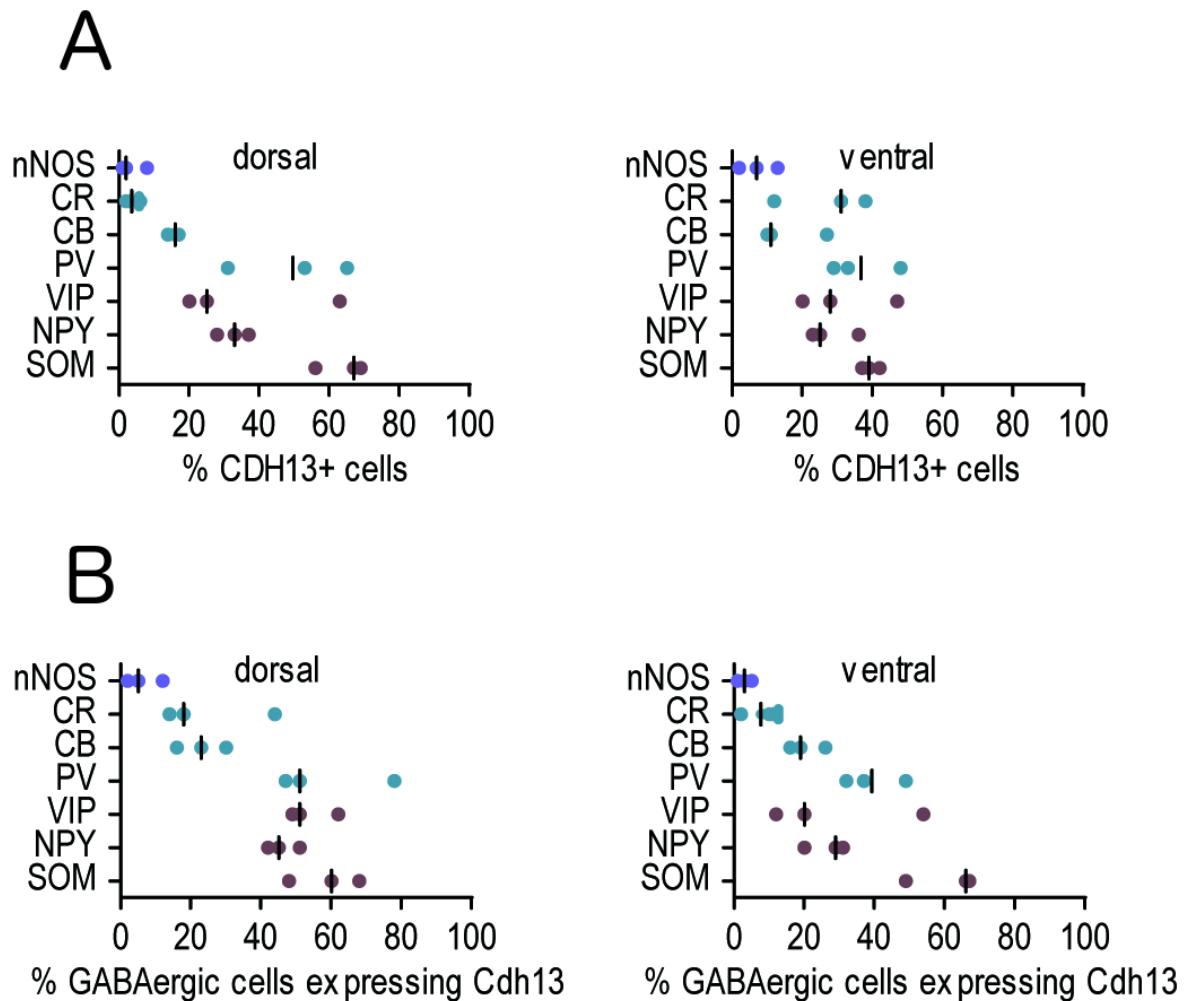

Figure 9: Colocalization of different chemical markers in CDH13-positive cells (A) and different marker cell populations (B). Blue dots: nNOS; turquoise dots: calcium-binding proteins; purple dots: neuropeptides. Abbreviations: PV, parvalbumin; NPY, neuropeptide Y; CB, calbindin; SOM, somatostatin, nNOS, nitric oxide synthase; CR, calretinin, VIP, vasoactive intestinal peptide. Reproduced from: Rivero, Selten et al. (2015), licensed under <u>CC BY 4.0</u>.

1.8 Transgenic animal models and *Cdh13* knockout mouse development

Transgenic animal models, first and foremost transgenic mouse models, have become an integral part of neuroscience research. Comparing knockout and wildtype individuals can provide valuable information regarding the function of a gene and its potential role in the etiology of a disease (Hermey 2011). To establish knockout models, different methods are available, such as embryonic stem (ES) cell targeting. In this method, an engineered

replacement vector can be transferred into cultured embryonic stem cells. The cells that have integrated the vector into their genome through homologous recombination are then injected into a blastocyst. Breeding of the chimera offspring leads to both homozygote and heterozygote knockout mice (Nobel Media AB 2014). This technology can be combined with the use of the Cre-loxP technology. It uses the enzyme Cre recombinase derived from bacteriophage P1 that deletes DNA within its specific target sequence loxP (= locus of X-over P1). These loxP sites can be inserted into the genome flanking the target genes, which are then referred to as "floxed" (= flanked by loxP) (Sauer 1987, Hermey 2011).

Constitutive *Cdh13* knockout mice (*Cdh13*^{-/-}) used in this thesis were created using this Cre-LoxP recombination system (Rivero, Selten et al. 2015). *Cdh13*[loxP/loxP] mice were crossed with a constitutive Cre deleter line, both in a C57Bl/6N background (Figure 10). To confirm the absence of CDH13 protein, western blots and immunohistochemistry were performed. *Cdh13* knockout mice show normal development, breeding and life expectancy.
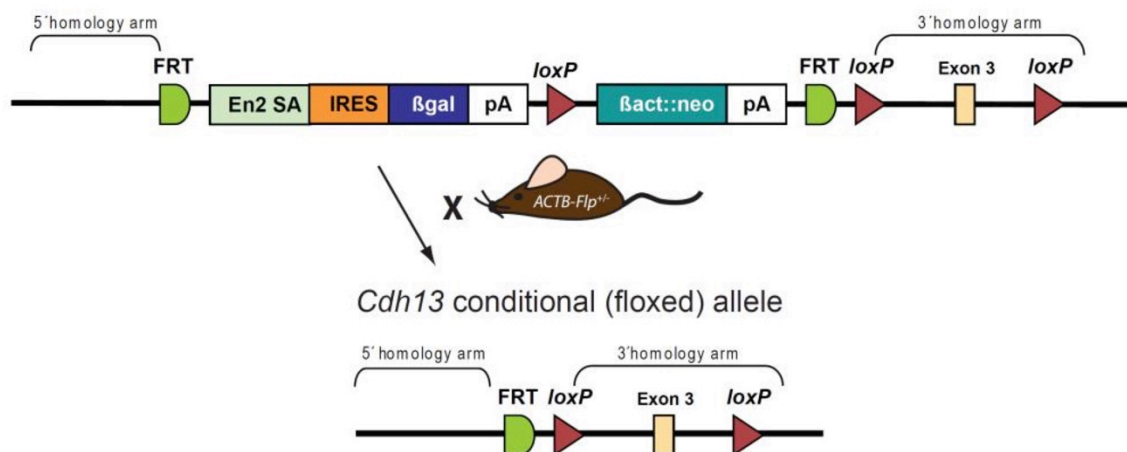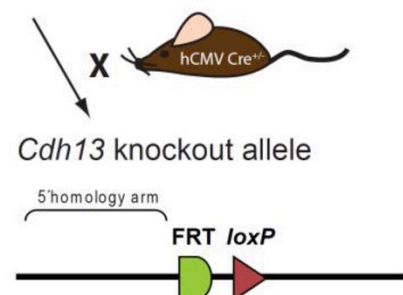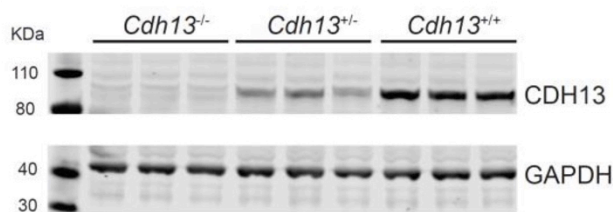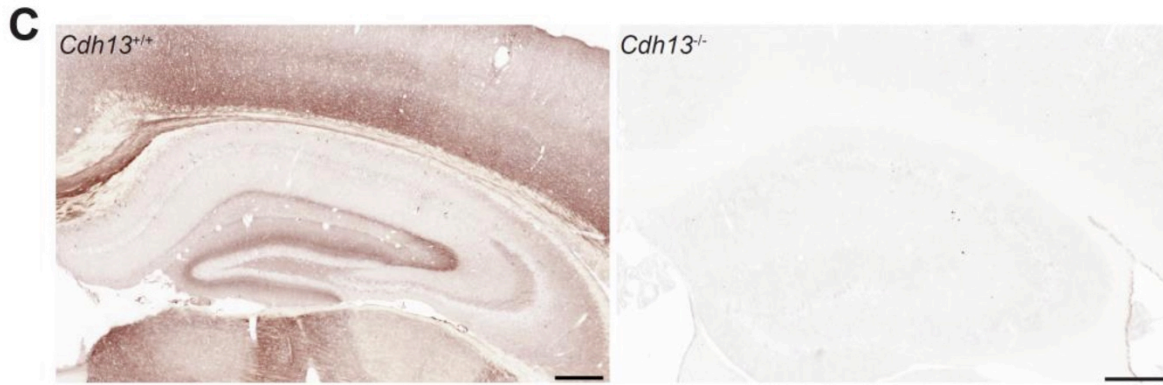
Figure 10: (A) Schematic representation of knockout construct. (B) Western blot analysis of different genotypes confirming the absence of CDH13 protein in knockout brain tissue, as well as a notable reduction in heterozygote (⁺/⁻) animals. (C) Immunohistochemistry also confirms the absence of CDH13 protein. No stained cells or fibers were found. Scale bars 300µm. Reproduced from Rivero, Selten et al. (2015), licensed under <u>CC BY 4.0</u>.

1.9 Objectives

CDH13 is an unconventional member of the cadherin superfamily of cell-adhesion molecules that has been identified by many GWAS as a risk gene for ADHD. Its unique structure suggests that it rather plays a role as a cellular receptor than a cell adhesion molecule. CDH13 shows a high level of colocalisation with PV-positive and SOM-positive GABAergic interneurons in the hippocampus, while its co-expression with nNOS is relatively low. This dissertation seeks to investigate the effect of CDH13 deficiency on these interneuron populations.

This study consists of two main projects: a stereological quantification of hippocampal PV-positive GABAergic interneurons among different genotypes was carried out to determine if CDH13 affects their formation. Additionally, a quantification of SOM-positive and nNOS-positive interneurons was executed in collaboration with Sarah Sich and Dmitrij Nagel. The second project was an assessment of the expression of genes involved in GABAergic and glutamatergic neurotransmission in the murine hippocampus among different genotypes to detect possible effects of CDH13 deficiency at the molecular level.

2. Materials and Methods

2.1 Animal husbandry, dissection and fixation

Mice were held in groups in the Zentrum für Experimentelle Molekulare Medizin of the University of Würzburg in a 12h day/night cycle with free access to food and water. For the sacrifice, mice were anaesthetized with isofluran and euthanized by cervical dislocation.

For the stereology study, native brains of adult mice (12-16 weeks of age) were dissected. 7-9 brains per genotype ($Cdh13^{-/-}$, $Cdh13^{+/-}$, $Cdh13^{+/+}$) were used for this purpose. After the dissection, brains were transferred into 50 ml tubes with 4% paraformaldehyde (PFA) (pH 6.5) in PBS and immersion-fixed at 4°C on a shaker for 48 h. Afterwards, the brains were cryoprotected by incubation in a 10% sucrose-solution for 24 hours at 4°C followed by another 48 h incubation in a 20% sucrose-solution at the same temperature. Finally, the brains were frozen in dry ice-cooled isopentane and stored at -80°C. At a later point, the brains were sectioned into 50 μ m coronal slices using a cryostat (Leica Mikrosysteme Vertrieb GmbH, Wetzlar, Germany). These sections included the whole dorsoventral hippocampus and were separated into 6 different series per brain. After sectioning, the sections were kept free-floating in a cryoprotectant solution.

For the qRT-PCR study, 10-12 brains per genotype of the same age group were dissected and immediately frozen in isopentane (-80°C). At a later stage, the brains were manually separated into different regions using an Olympus SZX7 stereo-microscope and a pre-cooled (-5°C) plate (Olympus, Hamburg, Germany). Afterwards, the whole hippocampi were transferred into RNase-free microcentrifuge tubes and stored at -80°C.

2.2 Immunohistochemistry

Immunochemistry is a widely used method to detect specific proteins in sectioned tissue. It uses monoclonal or polyclonal antibodies that bind specifically to one or several epitopes of the target protein. In a second step, these primary antibodies can then be visualized using either fluorescent molecules or enzymes bound to the antibody. As the concentration of the target protein is often very low, there are several methods to enhance the signal. The most common approach is to add a secondary antibody that binds the primary antibody on different sides. A further amplification can be reached by using the Avidin-Biotin-Complex (ABC). In

this process, the secondary antibody is bound to biotin (vitamin B7). Streptavidin, a glycoprotein with high biotin affinity, has 4 binding sites for biotin and therefore creates large reticular complexes of antibodies, biotin and streptavidin (Figure 11). The enzyme horseradish peroxidase (HRP) is also conjugated to the complex. After adding the enzyme substrates 3,3' diaminobenzidine tetrahydrochloride (DAB) and hydrogen peroxide (H_2O_2), DAB is oxidized to a brown polymer that is visible under the microscope.
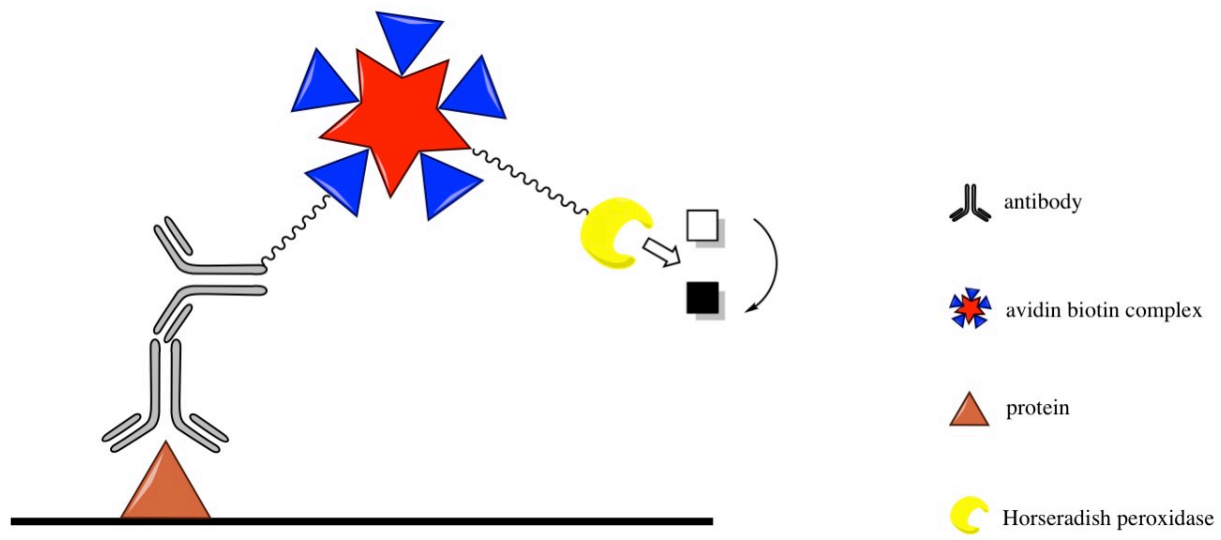

Figure 11: Indirect immunohistochemistry with secondary antibody and ABC. The marker molecule DAB is oxidized by conjugated HRP, leading to a brown precipitate at the site of the target protein. Adapted from: Hermey (2011).

2.2.1 Immunohistochemical staining

To prepare the brain tissue for staining, the previously cut free-floating slices were washed three times in 1x TBS for 5 min to remove the remaining cryoprotectant solution. Then the tissue was incubated in 0.6% hydrogen peroxide solution for 30 min to block endogenous peroxidase activity and reduce non-specific background staining. It was then washed in 1x TBS for 10 min, before being covered with citrate buffer and left at 80°C for 30 min for heat-induced epitope retrieval (HIER), which helps to reduce protein cross-linking in the target antigens. In the next step, the brain sections were incubated in blocking buffer for 90 min to further reduce unspecific staining. Afterwards, the slices were left in primary antibody solution containing anti-PV antibody for 48 h at 4°C.

In the second part of the staining process, the sections were washed three times in 1x TBS for 5 min and incubated in biotinylated goat anti rabbit antibody for 2 hours. After being washed again three times for 5 min in 1x TBS, the tissue was incubated in ABC for 90 min and

washed as described above. This amplifies the staining signal to a maximum degree by adding multiple avidin-biotin peroxidase complexes via the biotinylated secondary antibody to the antigen binding site (see above). The peroxidase is then developed by incubation with DAB solution for 6 min (DAB/metal concentrate (10x) diluted with peroxide buffer to a 1x solution according to the manufacturer's instructions). This results in a brown precipitate. The slices were then transferred into 1x TBS to stop the reaction, mounted on slides, left to dry and covered with the mounting medium Vitrocloud and cover slips. Negative controls included the substitution of the primary antibody with antibody diluent or pre-immune serum.

2.3. Stereology

Histological methods, such as immunohistochemistry, are most common approaches to investigate the structure of biological material. They are relatively easy to carry out and provide high-resolution images. However, creating two-dimensional images out of three-dimensional biological structures such as the brain, leads to a loss of structural information (Weibel, Kistler et al. 1966, West, Slomianka et al. 1991, West 2012). Stereology is a technique that "provides meaningful quantitative descriptions of the geometry of 3D structures from measurements that are made on 2D images" (West 2012). By measuring structural features of the sampled two-dimensional sections, it is possible to estimate the information from the lost dimension by using mathematical relationship equations (West 2012). Modern stereological methods are design-based and (statistically) unbiased. Unlike historical model-based counting techniques (Abercrombie 1946), sampling schemes and probes are designed in advance to be independent to structural changes within the tissue to be investigated. This eliminates potential bias, as wrong assumptions regarding the geometry of the tissue do not influence the results of the counting (Sterio 1984, Gundersen, Bagger et al. 1988, Gundersen, Bendtsen et al. 1988, West 2012, West 2012). Design-based stereology provides two methods to investigate the number of cells in a region of interest: the $N_V \times V_{REF}$ method and the optical fractionator method. The $N_V \times V_{REF}$ method uses an estimated reference volume V_{REF} of the region of interest and the numeric density of the counted object N_V to estimate the number of objects N (e.g. cells) in that region (West 2012).

$$N = N_V \times V_{REF}$$

The optical fractionator estimates the total number of objects N by counting the objects Q^- in a known fraction $1/f$ of the systematic randomly sampled reference volume (West 2012, West 2012).

$$N = \sum Q^- \times (1/f)$$

It uses section sampling fraction *ssf*, area sampling fraction *asf* and thickness sampling fraction *tsf* to calculate the fraction of the volume of the region sampled (Figure 12).
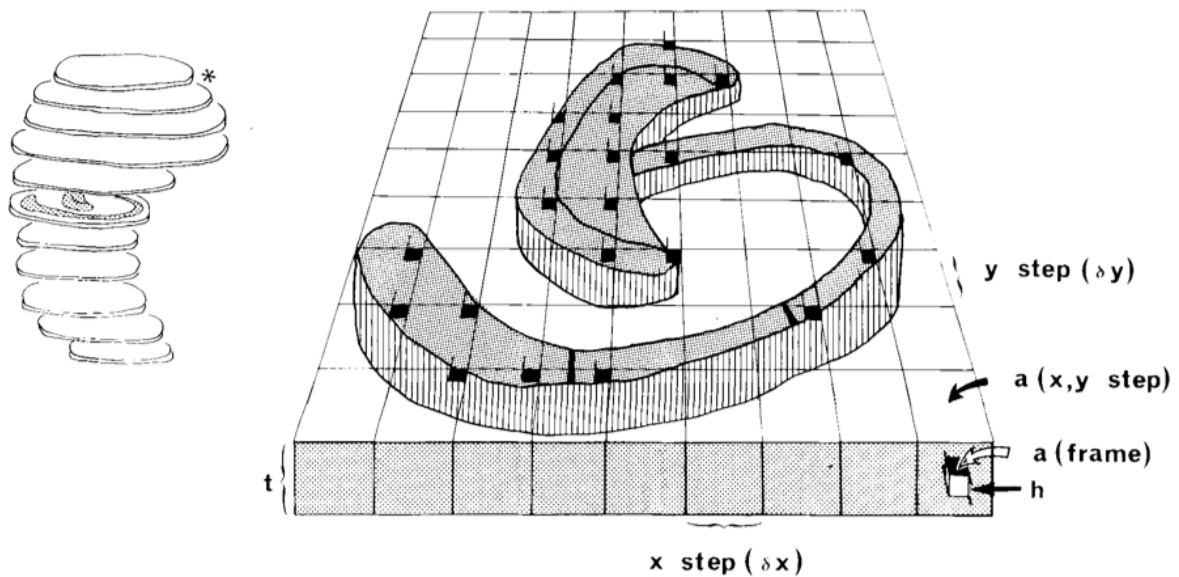
$$(1/f) = (1/ssf) \times (1/asf) \times (1/tsf)$$

Figure 12: Optical fractionator method in a rat hippocampus. Left image: systematic random sampling scheme. Right image: optical dissectors are applied to one section containing the region of interest. a(frame) is the counting frame, h the height of the optical dissector and a(x,y step) the area associated with each x,y movement of the microscope's motor (x step, y step). T is the thickness of the section. The thickness sampling fraction *tsf* is h/t. The area sampling fraction *asf* is (a(frame)/a(x,ystep)). The section sampling fraction *ssf* is the section interval. Reproduced from West, Slomianka et al. (1991) with permission from John Wiley and Sons.

2.3.1 Stereological study: quantification of immunolabeled neurons in the hippocampus

To quantify the number and density of GABAergic interneurons in the SO of the hippocampus, an Olympus BX51 microscope (Olympus, Hamburg, Germany) and Stereo Investigator imaging software v.11 (mbf Bioscience, Williston, VT, USA) were used. For the study, seven (*Cdh13*^{+/-}, *Cdh13*^{-/-}) or eight (*Cdh13*^{+/+}) DAB-stained brains of each genotype were analyzed using the optical fractionator workflow of the software. One systematic series of each brain was randomly selected, containing approximately nine representative sections of the whole hippocampus (Systematic Random Sampling: section sampling fraction *(ssf= 1/6)*.

Due to the low number of neurons in the area of interest, the area sampling fraction *(asf)* was set to one, therefore the whole section of interest was scanned for DAB-stained neurons. The other software parameters were set to: counting frame and grid: 150 μm x 150 μm, optical dissector height: 15 μm, top and bottom guard zones: 1.5 μm. Also number of section series and starting sections were defined. The SO was then selected as region of interest according to Allen Mouse Brain Atlas (Jones, Overly et al. 2009) and the sections were differentiated into anterior and posterior hippocampus in relation to the corpus callosum.

Cells inside the SO that showed typical neuron anatomy (soma and neurite) and were clearly marked during the DAB staining, were manually selected following the software workflow protocol. The data was then exported to Microsoft Excel (2011). The volume of the stratum oriens (mm^3) and the estimated population of stained cells were calculated by the stereology software using (amongst others) thickness of sections, number of sections and the section interval. The cell density (cells/mm^3) was calculated by dividing the population number by the volume in Excel. The statistical analysis between the different genotypes was then performed with Prism 6.04 (GraphPad Software, La Jolla, California, USA) by using the Kruskal-Wallis test. All slides were blind-coded by a third person until the analysis of all brains was finished.

2.4 Quantitative real-time polymerase chain reaction (qRT-PCR): quantification of genes involved in GABAergic and glutamatergic neurotransmission

PCR is the most common method for the amplification of DNA. It uses heat-stable *Taq* polymerase to replicate specific DNA sequences with the help of complementary primers. Typically, the PCR consists of 3 parts that are conducted in a thermal cycler. First, the double-strand DNA template is denatured by heating the cycler to 95°C. In the following annealing step, the temperature is lowered, so the primers can bind to their target regions in each of the DNA strands. In the elongation step, the DNA polymerase creates complementary DNA starting from the primers. Each run of the PCR amplifies the DNA template exponentially (Figure 13).

Quantitative real-time PCR is a modification of the classical approach. It combines the principle of conventional PCR with real-time detection of the amplification product and allows the calculation of relative gene expression levels. Special dyes, such as SYBR Green, bind directly to double-stranded DNA and produce a fluorescence signal that is detected by

the qRT-PCR machine in each cycle. Within the exponential amplification phase a threshold is set above the fluorescent baseline. The number of cycles needed by a gene to reach the threshold (C_q) allows the estimation of the relative gene expression of a target mRNA after normalisation to reference genes (Figure 14). In this study, the expression of 24 genes involved in GABAergic and glutamatergic neurotransmission was assessed and compared among genotypes. This included GABA-A receptor subunits, vesicular GABA and glutamate transporters and some of their interaction partners, GABA catalyzing enzymes and chemical markers of GABAergic interneurons.

For detection of gene expression levels, it is necessary to first extract and purify the RNA from the target tissue. After lysis, the solution is applied to a silica membrane that is able to bind RNA. After being washed and freed from impurities, the RNA is dissolved in water. As the PCR method works with a DNA polymerase, the RNA is transcribed into complementary Deoxyribonucleic Acid (cDNA) using a reverse transcriptase (RT) derived from a murine leukemia virus (MLV).
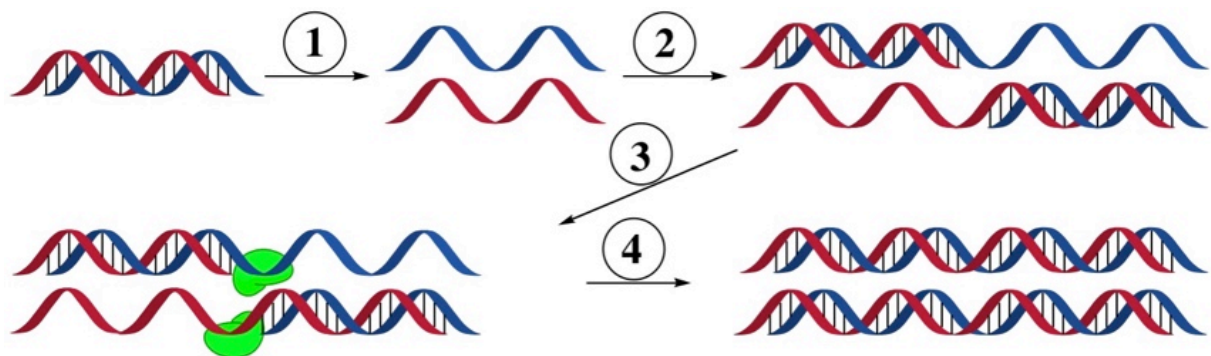

Figure 13: Schematic overview of a PCR. 1: Denaturation of the double strands. 2: Annealing of the primers. 3: Extension of the strands with DNA polymerase. 4: Amplified DNA template.
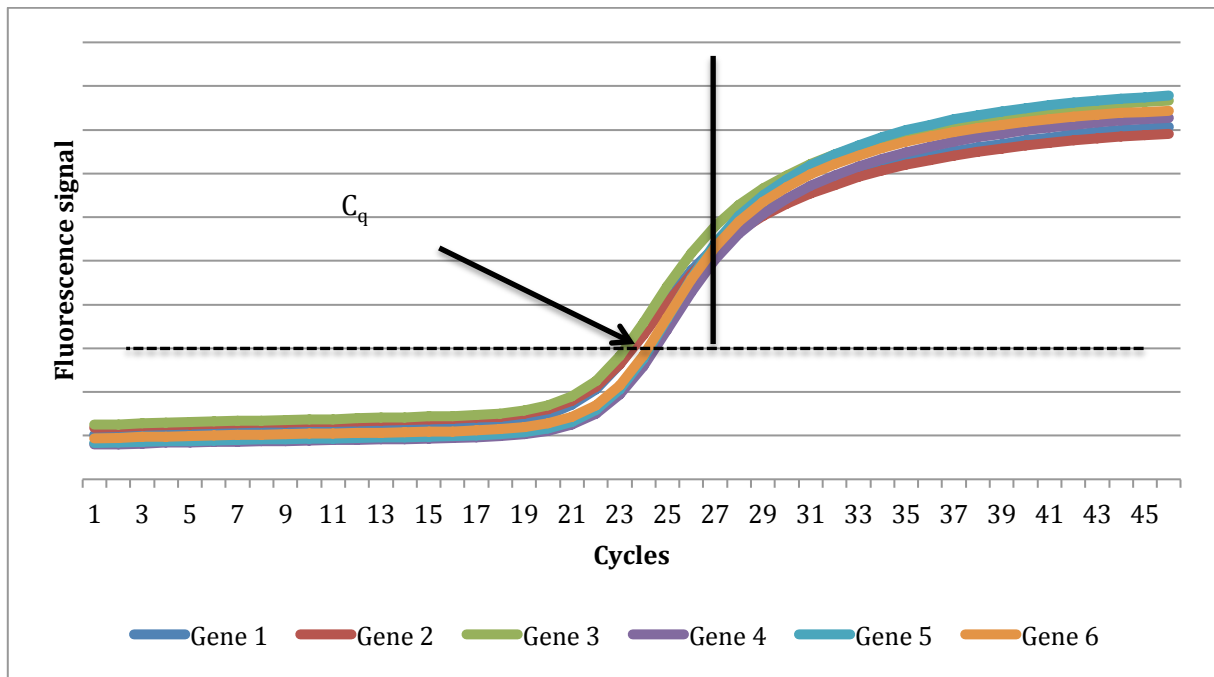
Figure 14: Amplification plot of a qRT-PCR with 6 genes. The horizontal dotted line indicates the fluorescence threshold. The vertical line indicates the transition from the exponential phase (left) to the plateau phase (right). The quantification cycle (C_q) indicates how many cycles are needed by a specific gene to reach the threshold.

2.4.1. Ribonucleic acid (RNA) isolation and processing

For the RNA isolation, miRNeasy Mini Kits (Qiagen, Venlo, Netherlands) were used. All reagents were part of the set, except where otherwise specified. Each of the 35 dissected and frozen hippocampi were placed in a sterile, RNase-free microcentrifuge together with a steel bead and 300 μl of Qiazol solution. It was then homogenized in the TissueLyser bead mill (Qiagen, Venlo, Netherlands) for 60 s at 20 Hz. The solution was then incubated for 5 min at room temperature and mixed with 60 μl chloroform for 15 s and incubated 10 min in ice. Afterwards, it was transferred to Maxtract-Tubes to be centrifuged for 5 min at 12000 xg at 17°C. The aqueous phase containing the nucleic acids was transferred into new tubes and mixed with 1.5 volumes of 100% ethanol. It was then transferred to a spin column and centrifuged at 12000 xg at 24°C for 15 s. For washing, 350 μl RWT buffer was added, centrifuged at 12000 xg for 15 s and discarded. Removal of genomic DNA was accomplished by the use of RNase-Free DNase Set (Qiagen, Venlo, The Netherlands). 80 μl of a mixture of 10 μl DNase and 70 μl RDD buffer was applied to the column and left incubating for 30 min. After discarding the flow-through and centrifugation at 12000 xg for 15 s, several washing steps followed:

- 350 μl RWT buffer pipetted onto column. Flow-through discarded. Centrifuged at 12000 xg for 15 s.

- 500 μl RPE buffer pipetted onto column. Flow-through discarded. Centrifuged at 12000 xg for 15 s.

- 500 μl RPE buffer pipetted onto column. Flow-through discarded. Centrifuged at 12000 xg for 2 min.

The column then was dried by 1 min of centrifugation at 12000 xg and placed into a new tube. 50 μl of DNase/RNase-free water was pipetted to the column, which was then centrifuged at 12000 xg for 1 min. The flow-through that contained the purified RNA was collected and stored at -80°C until further usage.

2.4.2. Complementary Deoxyribonucleic Acid (cDNA) Synthesis

Before cDNA synthesis, all RNA samples were tested with a NanoDrop spectrophotometer (Thermo Fisher Scientific, Waltham, Massachusetts, USA) for concentration and purity (Supplementary Table 1). In addition, both an agarose gel electrophoresis and the Experion™ Automated Electrophoresis System (Bio-Rad Laboratories, Inc., Hercules, California, USA) were used to assure good quality and integrity of the samples (Figure 15, 16 and 17). For the cDNA synthesis, iScript™ cDNA Synthesis Kits (Bio-Rad Laboratories, Inc., Hercules, California, USA) were used. All expendable material was part of the set, except where otherwise specified. According to the NanoDrop measurements, 1 μg of isolated RNA was diluted in 4 μl gDNA wipeout buffer. The solution was filled up with nuclease-free water until a total volume of 28 μl was reached. Together with 4 μl iScript reaction mix and 1 μl iScript reverse transcriptase, the RNA solution was added into sterile, nuclease-free tubes. The reaction protocol included the following steps in a thermal cycler:

- Priming: 5 min at 25°C

- Reverse transcription: 30 min at 42°C

- Inactivation of reverse transcription: 5 min at 85°C

The reaction was stopped by cooling down to 4°C. The synthesized cDNA was diluted 1:5 in 1x TE buffer, aliquoted and stored at -20°C.
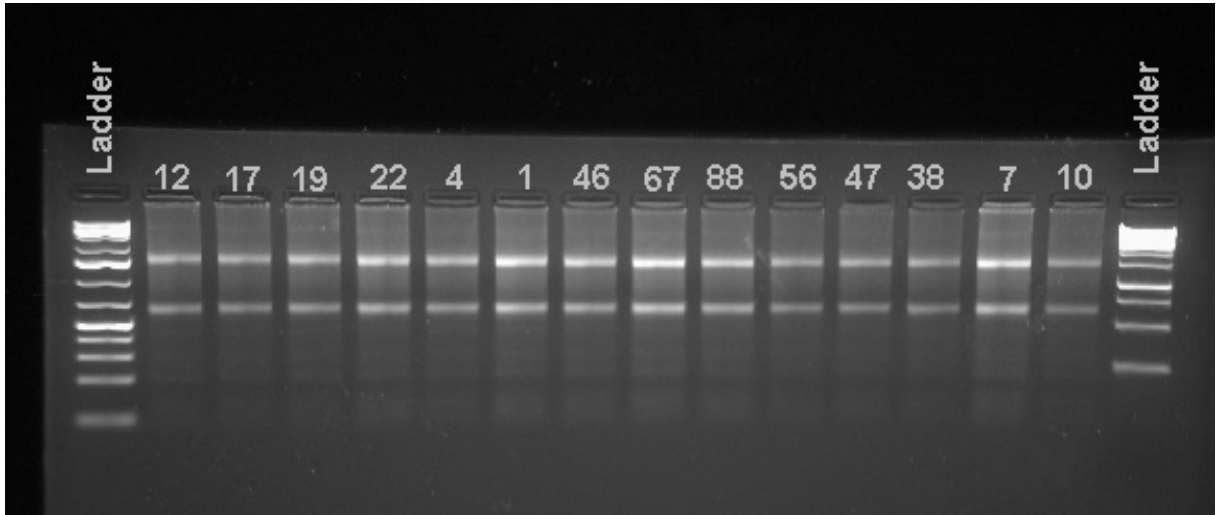
Figure 15: Agarose gel electrophoresis of RNA samples. Good visibility of the 28S and 18S bands of ribosomal RNA indicates good RNA quality.
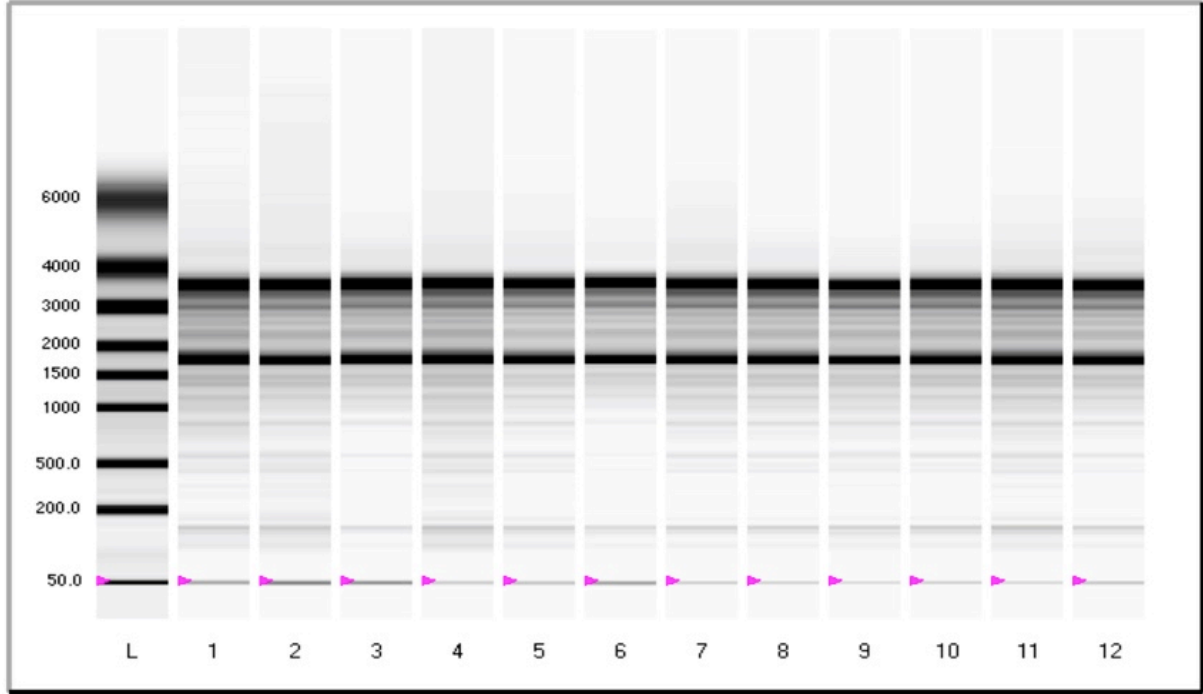

Figure 16: Virtual Gel Report of RNA samples with Experion system confirms the results of the gel electrophoresis.
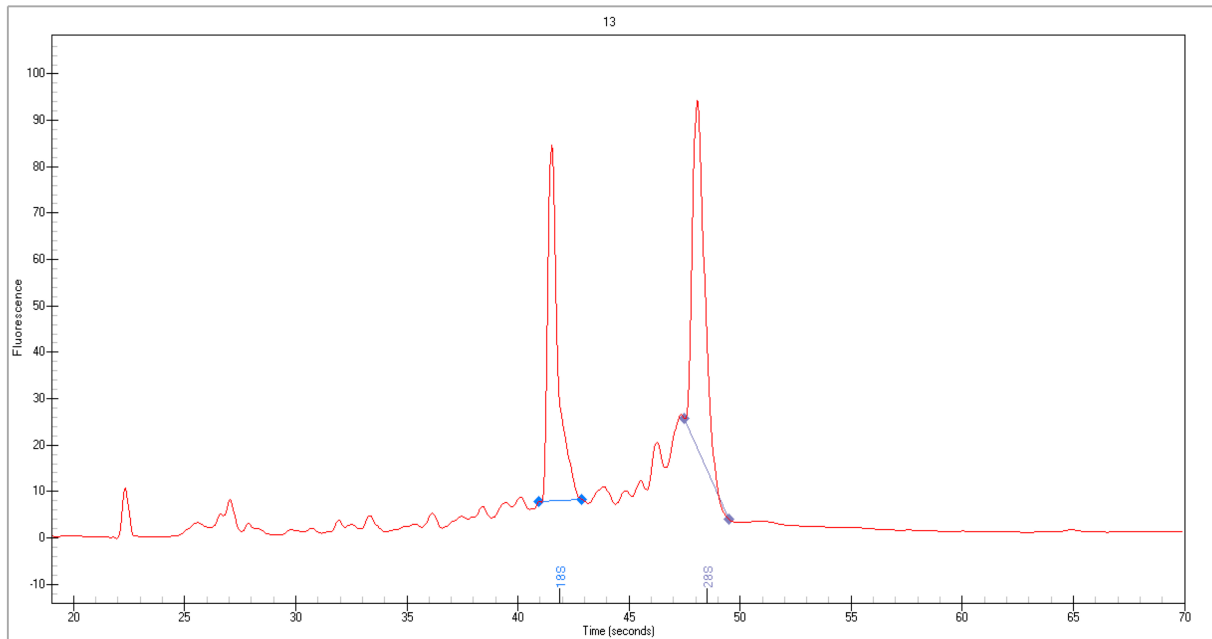
Figure 17: The two prominent peaks in the electropherogram of the Experion system represent 28S and 18S ribosomal RNA.

2.4.3. qRT-PCR, efficiency determination and statistical analysis

For the qRT-PCR, SYBR™ Select Master Mix for CFX (Thermo Fisher Scientific, Waltham, Massachusetts, USA) was used. Below it is referred to as SYBR Mix. Two mixes were prepared: one contained 5 μl SYBR Mix and 1 μl primer mix (both forward and reverse, 5 μM each - Qiagen, Venlo, Netherlands) and was then added into a 384-well PCR Plate (Bio-Rad Laboratories, Inc., Hercules, California, USA). The other mix contained 1 μl sample cDNA and 3 μl nuclease-free water. Each cDNA sample was analyzed in triplicate for each gene of interest. A negative control row with water instead of cDNA was added. The well layout was designed using CFX Manager™ (Bio-Rad Laboratories, Inc., Hercules, California, USA). Table 1 shows a characteristic well layout.

Cadherin-13	Cadherin-13	Cadherin-13	GAPDH	GAPDH	GAPDH	ACTB	ACTB	ACTB
Sample 1	Sample 1	Sample 1	Sample 1	Sample 1	Sample 1	Sample 1	Sample 1	Sample 1
U-2	U-2	U-2	U-5	U-5	U-5	U-8	U-8	U-8
Cadherin-13	Cadherin-13	Cadherin-13	GAPDH	GAPDH	GAPDH	ACTB	ACTB	ACTB
Sample 2	Sample 2	Sample 2	Sample 2	Sample 2	Sample 2	Sample 2	Sample 2	Sample 2
U-3	U-3	U-3	U-6	U-6	U-6	U-9	U-9	U-9
Cadherin-13	Cadherin-13	Cadherin-13	GAPDH	GAPDH	GAPDH	ACTB	ACTB	ACTB
Sample 3	Sample 3	Sample 3	Sample 3	Sample 3	Sample 3	Sample 3	Sample 3	Sample 3
N	N	N	N	N	N	N	N	N
Cadherin-13	Cadherin-13	Cadherin-13	GAPDH	GAPDH	GAPDH	ACTB	ACTB	ACTB
H2O	H2O	H2O	H2O	H2O	H2O	H2O	H2O	H2O

Table 1: Representative section of a 384-well layout. Each row contained cDNA from a different hippocampus sample. Each sample is tested in triplicate for each gene. The last row contains water as negative control. Exported from CFX Manager™ (Bio-Rad Laboratories, Inc., Hercules, California, USA).

The plate was covered, centrifuged, placed into a CFX384 thermal cycler (Bio-Rad Laboratories, Inc., Hercules, California, USA) and the "Standard Cycling Mode" protocol was run in the CFX Manager™ software. PCR efficiency determination was performed using LinRegPCR (Ramakers, Ruijter et al. 2003) with raw (not baseline-corrected) PCR data according to (Ruijter, Ramakers et al. 2009). qbase+ qRT-PCR analysis software (Biogazelle, Zwijnaarde, Belgium) was used for calculation of the gene expression values for each sample and target gene. Specifically gene expression values were normalized using a combination of the most stable reference genes as well as the calculated efficiency values for each amplicon. The statistical analysis was then performed using the Kruskal-Wallis test, which was implemented in Prism 6.0 (GraphPad Software, La Jolla, California, USA). In case significant differences among genotypes were found, Tukey's multiple comparisons test was used as a post-hoc test.

2.5 List of materials

2.5.1. Immunohistochemistry

Antibodies

Primary antibodies

Antibody	Contributor	Concentration used
Anti-PV, made in rabbit	Swant Marly, Switzerland	1:12000
Anti-SOM, made in rat	Merck Millipore, Burlington, Massachusetts, USA	1:1000
Anti-nNOS, made in rabbit	Merck Millipore, Burlington, Massachusetts, USA	1:6000

Secondary antibodies

Antibody	Contributor	Concentration used
Biotinylated anti Rabbit IgG, made in goat	Vector laboratories, Burlingame, California, USA	1:1000
Biotinylated anti Rat IgG, made in goat	Vector laboratories, Burlingame, California, USA	1:1000

Kits

Name	Contributor
ABC Kit	Vector laboratories, Burlingame, California, USA
DAB Substrate Kit	Roche Diagnostics, Risch-Rotkreuz, Switzerland

Reagents

Name	Contributor
Cryo-Gel	Leica Biosystems, Nussloch, Germany
D(+)-Sucrose	AppliChem, Darmstadt, Germany
Ethylene Glycol	Sigma Aldrich, St. Louis, Missouri, USA
Glycerin	AppliChem, Darmstadt, Germany
Hydrogen peroxide 30%	Merck, Darmstadt, Germany
Isoflurane	cp-pharma, Burgdorf, Germany
Isopentane	AppliChem, Darmstadt, Germany
Normal goat serum	Vector Laboratories, Burlingame, California, USA
Normal horse serum	Vector Laboratories, Burlingame, California, USA
Paraformaldehyde	Carl Roth, Karlsruhe, Germany
Phosphate buffered saline (10x)	Lonza Group, Basel, Switzerland
Sodium chloride	Sigma Aldrich, St. Louis, Missouri, USA
Tri-Sodium citrate	Sigma Aldrich, St. Louis, Missouri, USA
Triton X-100	Sigma Aldrich, St. Louis, Missouri, USA
Vitro-Cloud	R. Langenbrinck, Emmendingen, Germany

Buffers and solutions

Solution	Production
1x TBS (tris-buffered saline; pH 7,5)	100 mM Tris-HCL 150 mM NaCl in ddH$_2$O
1x PBS (phosphate buffered saline)	1:10 dilution of 10xPBS in ddH$_2$O
4% PFA (pH 6,5)	PFA in 1x PBS
10% Sucrose solution	Sucrose in 1x PBS
20% Sucrose solution	Sucrose in 1x PBS
Cryoprotectant	25% glycerin 30% ethylene glycol in 1x TBS
10 mM sodium citrate buffer, pH 8,5	Tri-sodium-citrate in ddH$_2$O
Immunochemistry blocking buffer	10% NGS 0.25% Triton X-100 in 1x TBS
Primary antibody solution	5% NGS 0.25% Triton X-100 1x TBS
Secondary antibody solution	3% NGS 0.25% Triton X-100 1x TBS

Software

Name	Contributor
Stereo Investigator imaging software v.11	mbf Bioscience, Williston, Vermont, USA
Prism 6.04	GraphPad Software, La Jolla, California, USA
Microsoft Excel (2011)	Microsoft, Redmond, Washington, USA

2.5.2. qRT-PCR

RNA isolation

Reagents

Name	Contributor
miRNeasy Mini Kit	Qiagen, Venlo, Netherlands
Maxtract-Tubes High Density 1.5ml	Qiagen, Venlo, Netherlands
Stainless Steel Beads	Qiagen, Venlo, Netherlands
RNase-Free DNase Set	Qiagen, Venlo, Netherlands
Chloroform	Karl Roth, Karlsruhe, Germany

cDNA synthesis

Reagents

Name	Contributor
iScript™ cDNA Synthesis Kit	Bio-Rad Laboratories, Inc. Hercules, California, USA
1x TE buffer	AppliChem, Darmstadt, Germany

qRT-PCR

Reagents

Name	Contributor
SYBR™ Select Master Mix for CFX	Thermo Fisher Scientific, Waltham, Massachusetts, USA
QuantiTect Primer Assays	Qiagen, Venlo, Netherlands

Primer oligonucleotide sequences for target genes (metabion international AG, Planegg/Steinkirchen, Germany)

Gene	Gene (short)	Forward Primer (5'→3')	Reverse Primer (5'→3')	Amplicon size
GABA(A) Receptor, Alpha-1	*Gabra1*	gcccactaaaattcggaagc	cttctgctacaaccactgaacg	93 nt
GABA(A) Receptor, Alpha-2	*Gabra2*	acaaaaagaggatgggcttg	tcatgacggagcctttctct	73 nt
GABA(A) Receptor, Alpha-3	*Gabra3*	cttgggaaggcaagaaggta	tggagctgctggtgttttct	62 nt
GABA(A) Receptor, Alpha-4	*Gabra4*	aaagcctcccccagaagtt	catgttcaaattggcatgtgt	91 nt
GABA(A) Receptor, Alpha-5	*Gabra5*	gacggactcttggatggcta	acctgcgtgattcgctct	65 nt
GABA(A) Receptor, Beta-1	*Gabrb1*	ccctctggatgagcaaaact	aattcgatgtcatccgtggta	69 nt
GABA(A) Receptor, Beta-2	*Gabrb2*	gggtctccttttggattaactatga	ggtcattgttaggacagttgtaattc	77 nt
GABA(A) Receptor, Beta-3	*Gabrb3*	ctccattgtagagcaccgtct	tcaatgaaagtcgaggataggc	74 nt
GABA(A) Receptor, Gamma-1	*Gabrg1*	gaggcaggaagctgaaaaac	tgctgttcatgggaatgaga	78 nt
GABA(A) Receptor, Gamma-2	*Gabrg2*	acagaaaatgacgctgtgga	catctgactttttggcttgtgaa	71 nt
GABA(A) Receptor, Gamma-3	*Gabrg3*	ctgcttctcctctgcctgtt	ttctggtttgatggggagtc	89 nt
Gephyrin	*Gphn*	tgatcttcatgctcagatcca	gcaaatgttgttggcaagc	66 nt
Vesicular GABA Transporter	*Vgat, Slc32a1*	acgtgacaaatgccattcag	tgaggaacaaccccaggtag	84 nt
Glutamate Decarboxylase 1	*Gad1 (Gad67)*	atacaacctttggctgcatgt	ttccgggacatgagcagt	60 nt
Glutamate Decarboxylase 2	*Gad2 (Gad65)*	tgtagctgacatctgcaaaaagta	gggacatcagtaaccctcca	77 nt

Vesicular Glutamate Transporter	*Vglut, Slc17a7*	gtgcaatgaccaagcacaag	agatgacaccgccgtagtg	61 nt
Post-Synaptic Density Protein 95	*Psd95, Dlg4*	tctgtgcgagaggtagcaga	cggatgaagatggcgatag	110 nt
Tropomyosin-Related Kinase B	*TrkB, Ntrik2*	aaagcaatcgggagcatct	ccaacttgagcaggagcaac	96 nt
Parvalbumin	*Pvalb*	ttctggacaaagacaaaagtgg	tgaggagaagcccttcagaat	71 nt
Somatostatin	*Sst*	cccagactccgtcagtttct	gggcatcattctctgtctgg	118 nt
Serotonin Receptor 3A	*Htr3a*	ggtccctgacatcctcatca	cacgtacacataaggaatgttcg	70 nt
Brain Derived Neurotrophic Factor (exon IV splice variant)	*Bdnf*	gatccgagagctttgtgtgg	aaccatagtaaggaaaaggatggtc	76 nt
Brain Derived Neurotrophic Factor (exon I splice variant)	*Bdnf*	agtctccaggacagcaaagc	tgcaaccgaagtatgaaataacc	94 nt

Reference genes (QuantiTect Primer Assays, Qiagen, Venlo, Netherlands)

Gene	Gene (short)	Product Name (Qiagen)
ß-actin	*Actb*	Mm_Actb_1_SG
Glyceraldehyde 3-phosphate dehydrogenase	*Gapdh*	Mm_Gapdh_3_SG
Ubiquitin C	*Ubc*	Mm_Ubc_1_SG
Ribosomal protein, large, P0	*Rplp0*	Mm_Rplp0_1_SG
Beta-2 microglobulin	*B2m*	Mm_B2m_2_SG
Phosphoglycerate kinase 1	*Pgk1*	Mm_Pgk1_1_SG

Software

Name	Contributor
NanoDrop ND-1000 3.7	Thermo Fisher Scientific, Waltham, Massachusetts, USA
CFX Manager 3.0	Bio-Rad Laboratories, Inc. Hercules, California, USA
LinRegPCR, v. 2014.4	Heart Failure Research Center, Amsterdam, Netherlands
qBase+, v. 3.0	Biogazelle NV, Zwijnaarde, Belgium
Prism 6.04	GraphPad Software, La Jolla, California, USA

3. Results

3.1 Stereological quantification

A stereological quantification was carried out to investigate the influence of CDH13 deficiency on PV-positive interneurons in the SO of the murine hippocampus. Additionally, the influence on SOM-positive and nNOS-positive interneurons was assessed in collaboration with Sarah Sich and Dmitrij Nagel. The obtained data included the volume of the SO (mm^{3}), the estimated number of immunolabeled cells and their density (cells/mm^{3}). These data were obtained for the complete hippocampus, but also for the ventral and dorsal hippocampus separately, due to their functional differences. Figure 18 shows a representative section of the posterior hippocampus with a magnification of the SO with immunolabeled PV-positive cells.
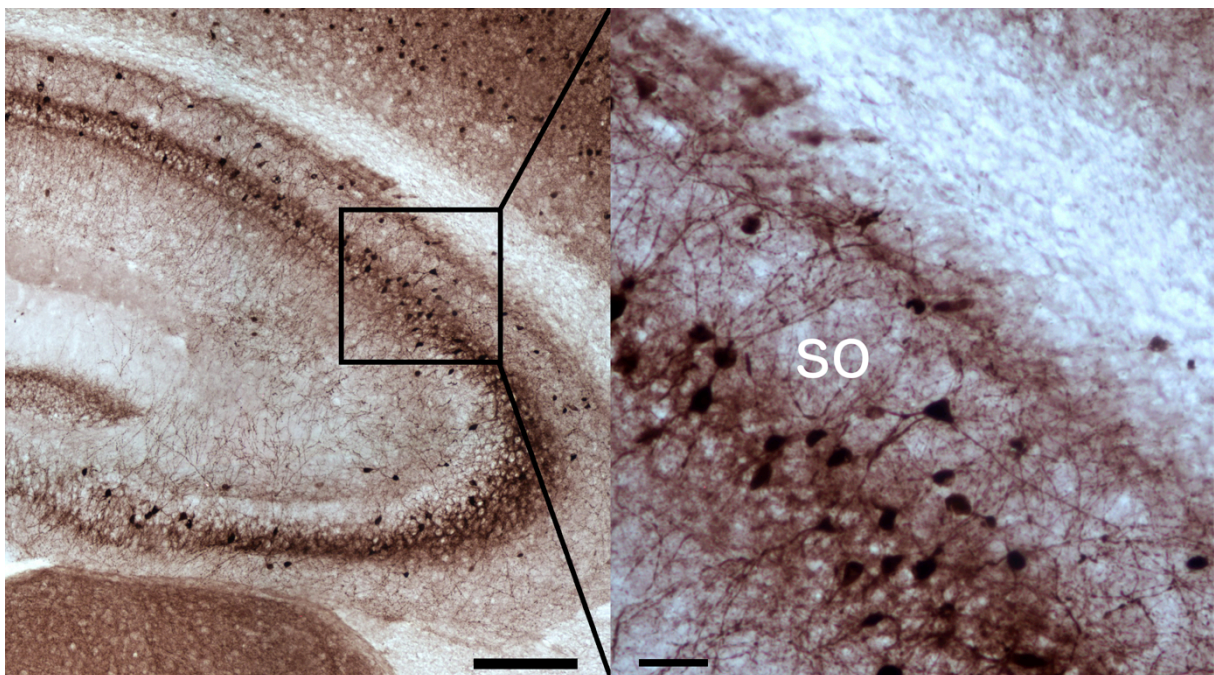

Figure 18: DAB-stained slice of the posterior hippocampus. PV-positive cells appear as dark brown precipitate. Scale bars: 200 µm (left) and 100 µm (right); so = stratum oriens.

3.1.1. Effect of CDH13 deficiency on the volume of the stratum oriens

The volume of ventral and dorsal hippocampus was very similar. The statistical analysis of all stained brains revealed no significant differences in the volume of the SO among different genotypes in the Kruskal-Wallis test (P > 0.05) (Figure 19).
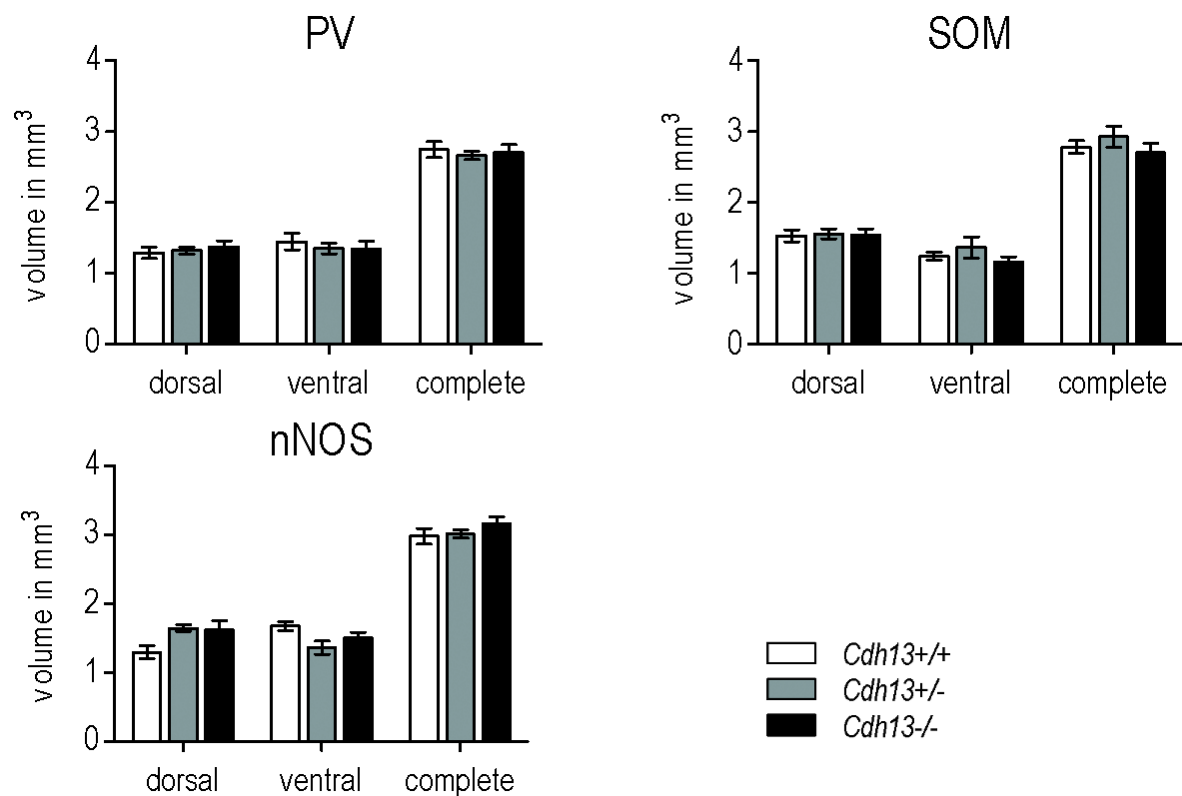

Figure 19: Stereological quantification of the volume of the SO among different genotypes and stainings. PV- stained brains on the left, SOM in the top right and nNOS on the bottom left. The bars represent mean SO volume. Error bars represent SEM. Kruskal-Wallis test revealed no significant differences between genotypes. (PV: *n= 8 Cdh13$^{+/+}$, 7 Cdh13$^{+/-}$, 7 Cdh13$^{-/-}$; SOM/nNOS: n=9 Cdh13$^{+/+}$, 8 Cdh13$^{+/-}$, 7 Cdh13$^{-/-}$*). SOM data obtained in collaboration with Sarah Sich, nNOS data obtained in collaboration with Dmitrij Nagel. Adapted from: Rivero, Selten et al. (2015), licensed under <ins>CC BY 4.0</ins>.

3.1.2. Effect of CDH13 deficiency on PV-positive cells in the stratum oriens of the hippocampus

In the PV-stained brains, both the estimated cell population and the cell density showed no genotype-dependent differences in the Kruskal-Wallis test (P > 0.05) (Figure 20).
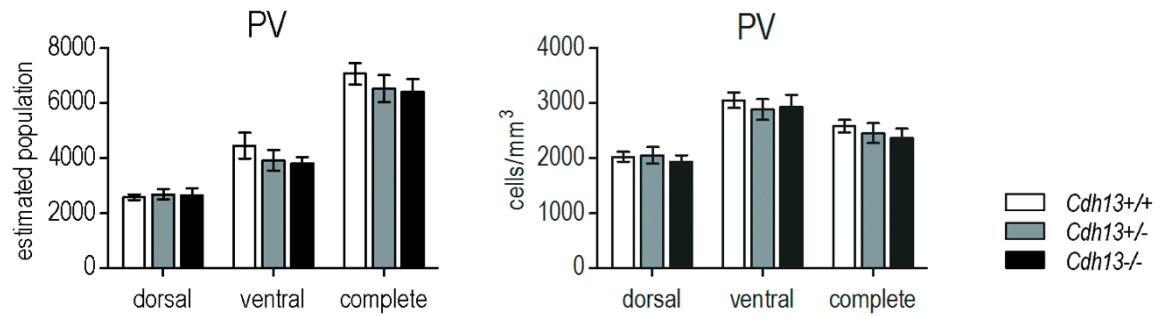
Figure 20: Stereological quantification of the estimated population (left) and cell density (right) of PV-positive cells in the SO of the hippocampus. The bars represent mean SO volume. Error bars represent SEM. Kruskal-Wallis test revealed no significant differences between genotypes. (*n= 8 Cdh13+/+, 7 Cdh13+/-, 7 Cdh13-/-*). Adapted from Rivero, Selten et al. (2015), licensed under <u>CC BY 4.0.</u>

3.1.3. Effect of CDH13 deficiency on SOM-positive cells in the stratum oriens of the hippocampus

In SOM-stained brains, no genotype-dependent differences in the estimated cell population and cell density were found using the Kruskal-Wallis test ($P > 0.05$) (Figure 21).

Figure 21: Stereological quantification of the estimated population (left) and cell density (right) of SOM-positive cells in the SO of the hippocampus. The bars represent mean SO volume. Error bars represent SEM. Kruskal-Wallis test revealed no significant differences between genotypes. (*n=9 Cdh13+/+, 8 Cdh13+/-, 7 Cdh13-/-*). SOM data obtained with Sarah Sich. Adapted from: Rivero, Selten et al. (2015), licensed under <u>CC BY 4.0</u>**.**

3.1.4. Effect of CDH13 deficiency on nNOS-positive cells in the stratum oriens of the hippocampus

The analysis of the nNOS-stained brains revealed only minimal differences in the estimated cell population and cell density. None of these differences were statistically significant in the Kruskal-Wallis test either ($P > 0.05$) (Figure 22).
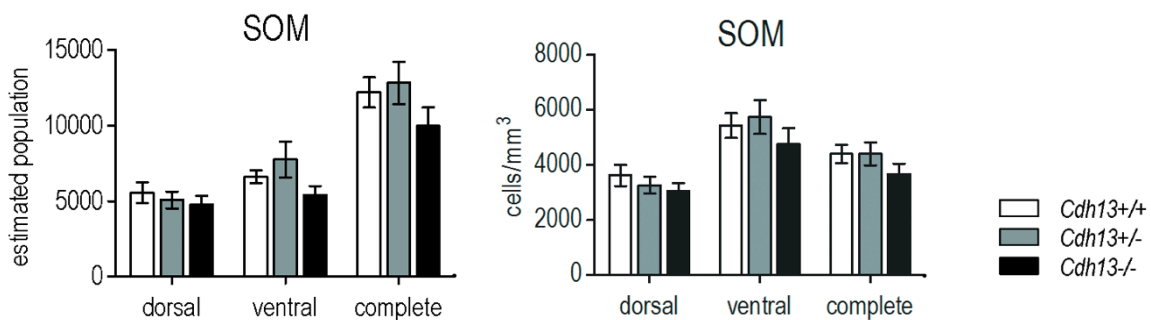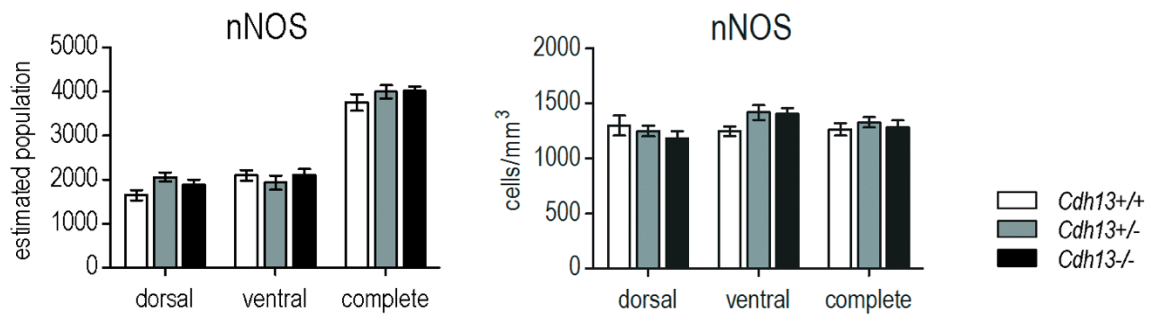
Figure 22: Stereological quantification of the estimated population (left) and cell density (right) of nNOS-positive cells in the SO of the hippocampus. The bars represent mean SO volume. Error bars represent SEM. Kruskal-Wallis test revealed no significant differences between genotypes. ($n=9$ Cdh13+/+, 8 Cdh13+/-, 7 Cdh13-/-). nNOS data obtained with Dmitrij Nagel. Adapted from: Rivero, Selten et al. (2015), licensed under <u>CC BY 4.0</u>.

3.2 Gene expression analysis

qRT-PCR was carried out to investigate the influence of CDH13 deficiency on the mRNA expression of genes involved in GABAergic and glutamatergic neurotransmission, including GABA-A receptor subunits, vesicular GABA and glutamate transporters and some of their interaction partners, GABA catalyzing enzymes and chemical marker of GABAergic interneurons.

3.2.1. Effects on the GABAergic system

Post-synaptic GABAergic genes: GABA-A receptors and interaction partners

The gene expression analysis of the GABA-A receptor alpha subunits revealed only minimal changes among genotypes. No significant threshold was reached using the Kruskal-Wallis test ($P > 0.05$) (Figure 23).

Figure 23: Normalized expression of GABA A receptor subunits alpha *Gabra1, Gabra2, Gabra3, Gabra4, Gabra5* in the hippocampus. The bars represent mean normalized expression. Error bars represent SEM. Kruskal-Wallis test revealed no significant differences between genotypes (n=9-12 per genotype).

Analysis of GABA-A receptor beta subunits also yielded very similar normalized expression among genotypes. No statistical significance in the Kruskal-Wallis test was reached (Figure 24).
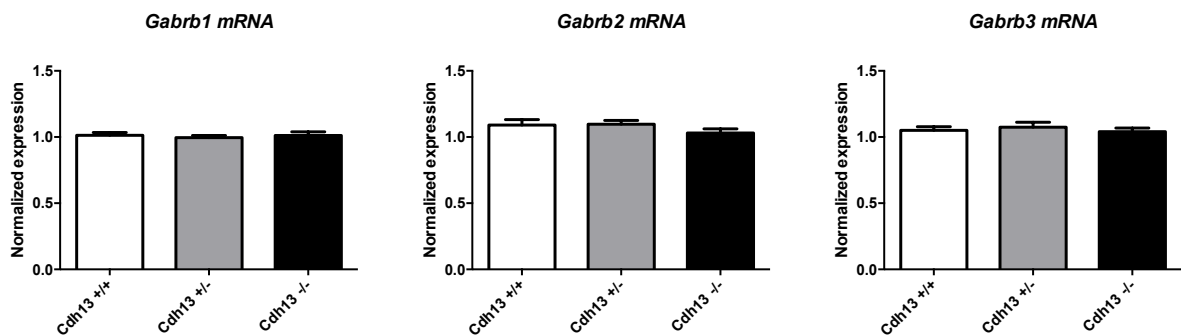
Figure 24: Normalized expression of GABA A receptor subunits beta *Gabrb1, Gabrb2, Gabrb3* in the hippocampus. The bars represent mean normalized expression. Error bars represent SEM. Kruskal-Wallis test revealed no significant differences between genotypes. (n=10-12 per genotype)

Expression of GABA A receptor gamma subunits continued the trend of the two other GABA-A receptor subtypes that were analyzed in this study. They also showed only minimal differences among genotypes that did not reach significance (Figure 25).
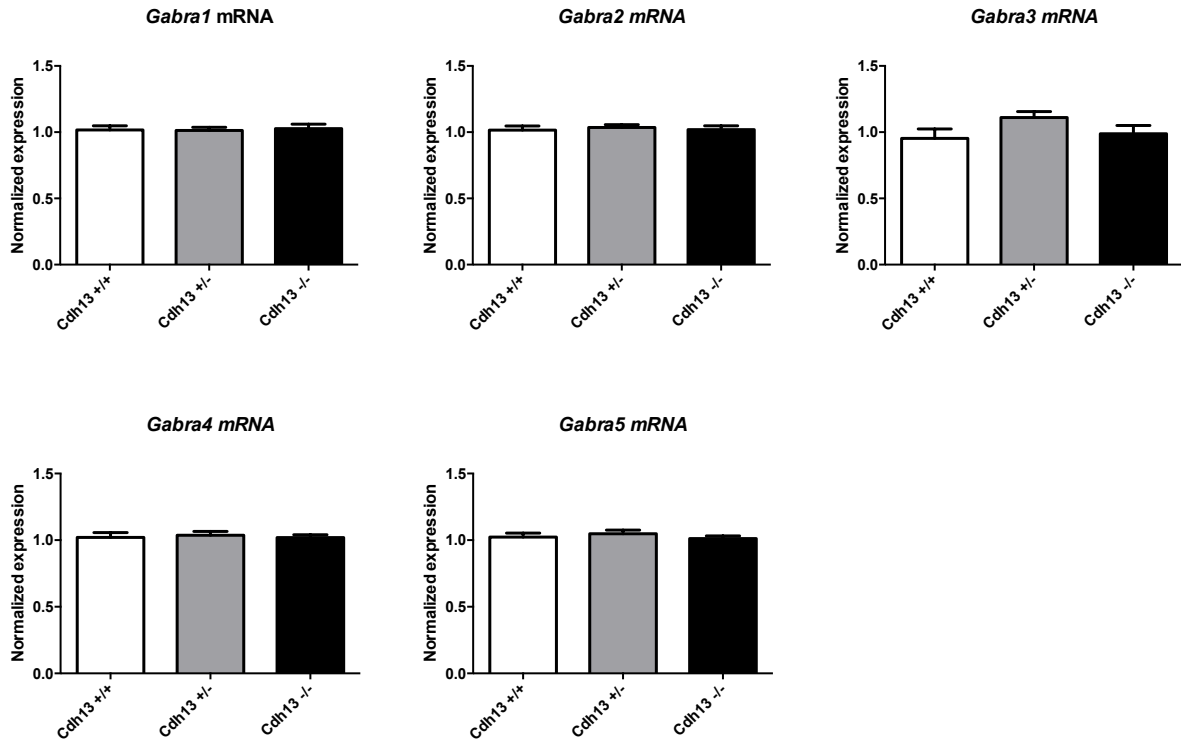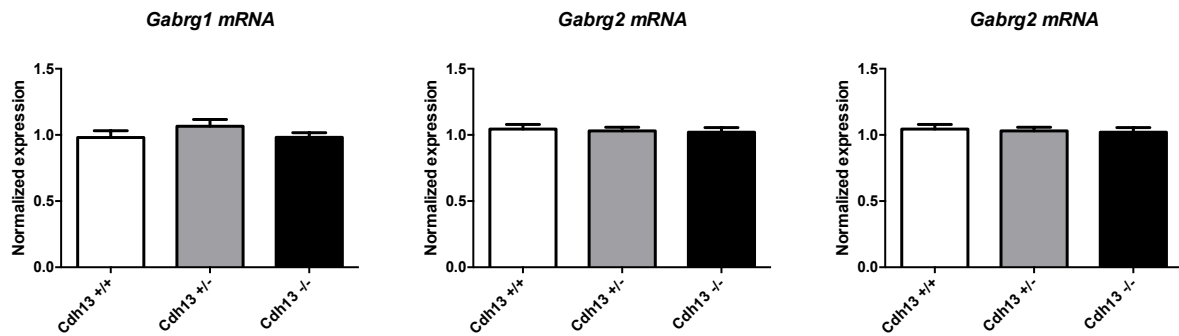

Figure 25: Normalized expression of GABA A receptor subunits gamma *Gabrg1*, *Gabrg2*, *Gabrg3* in the hippocampus. The bars represent mean normalized expression. Error bars represent SEM. Kruskal-Wallis revealed no significant differences between genotypes. (n=9-12 per genotype)

GABA A receptor partner gephyrin only showed minimal differences among genotypes that were not statistically significant in the Kruskal-Wallis test (Figure 26).
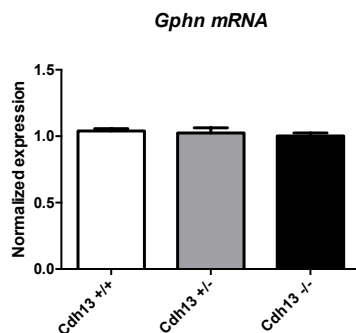
Figure 26: Normalized expression of Gephyrin (*Gphn*) in the hippocampus. The bars represent mean normalized expression. Error bars represent SEM. Kruskal-Wallis revealed no significant differences between genotypes. (n=9-12 per genotype)

Enzymes catalyzing GABA synthesis

The gene expression analysis of glutamate decarboxylases revealed no genotype-dependent differences that reached significant threshold in the Kruskal-Wallis test (Figure 27).
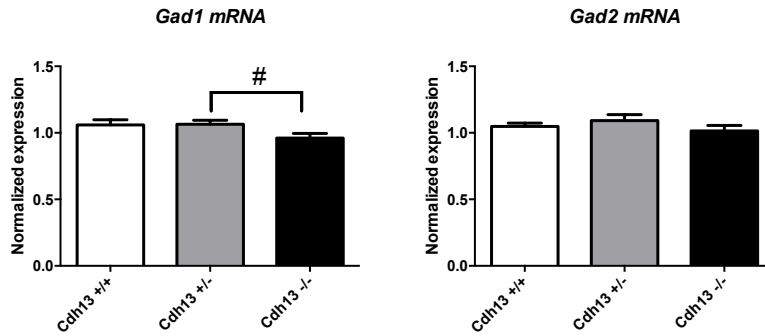
Figure 27: Normalized expression of the GABA synthesizing enzyme glutamate decarboxylase *Gad1, Gad2* **in the hippocampus. The bars represent mean normalized expression. Error bars represent SEM. Kruskal-Wallis test revealed no significant differences between genotypes. (n=9-12, #P <0.1)**

GABA Transporter

Although the differences in the expression of the vesicular GABA transporter appeared to be greater than in the samples described previously, no significant threshold was reached in the Kruskal-Wallis test (Figure 28).
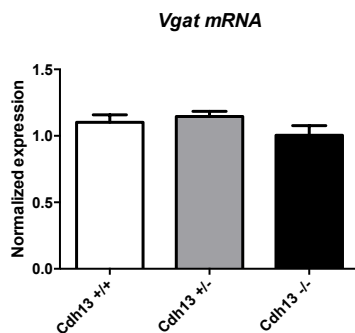
Figure 28: Normalized expression of the vesicular GABA transporter *Vgat* **. The bars represent mean normalized expression. Error bars represent SEM. Kruskal-Wallis test revealed no significant differences between genotypes. (n=9-12 per genotype)**

BDNF pathway genes

The gene expression analysis of brain derived neurotrophic factor splice variants *BdnfI* and *BdnfIV* did not reveal any genotype-dependent differences.

On the other hand, the Kruskal-Wallis test revealed significant differences among genotypes in *TrkB* expression (P = 0.0156). Tukey's multiple comparisons test indicated significant differences between *Cdh13*$^{+/+}$ and *Cdh13*$^{-/-}$ mice (adjusted P = 0.0075) and also between *Cdh13*$^{+/-}$ and *Cdh13*$^{-/-}$ mice (adjusted P = 0.0148), with *Cdh13*$^{-/-}$ animals showing the lowest gene expression levels (Figure 29).
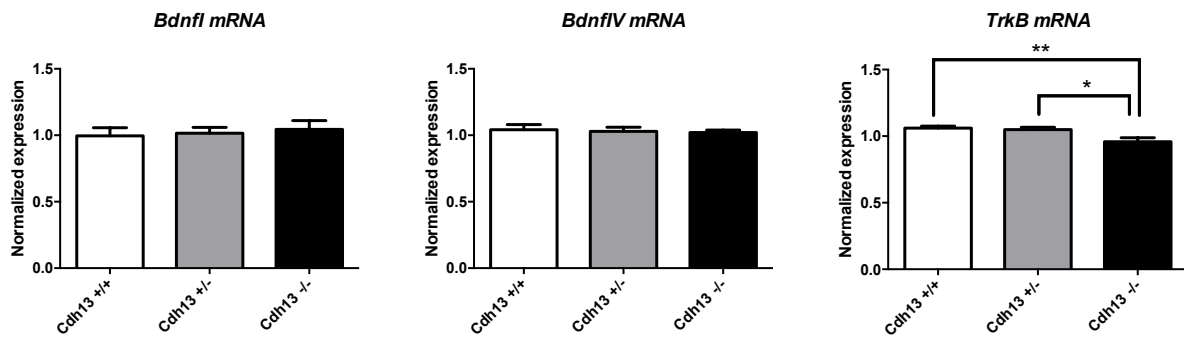
Figure 29: Normalized expression of the brain derived neurotrophic factor splice variants *BdnfI, BdnfI* and the BDNF-receptor *TrkB* in the hippocampus. The bars represent mean normalized expression. Error bars represent SEM. *TrkB* expression was significantly lower in ko mice. The other genes showed no significant differences between genotypes in the Kruskal-Wallis test. (n=10-12 per genotype, **P < 0.01, *P<0.05)

GABA interneuron markers

Analysis of the chemical interneuron markers Parvalbumin, Somatostatin and serotonin receptor 3A revealed no statistically significant differences among genotypes (Figure 30).
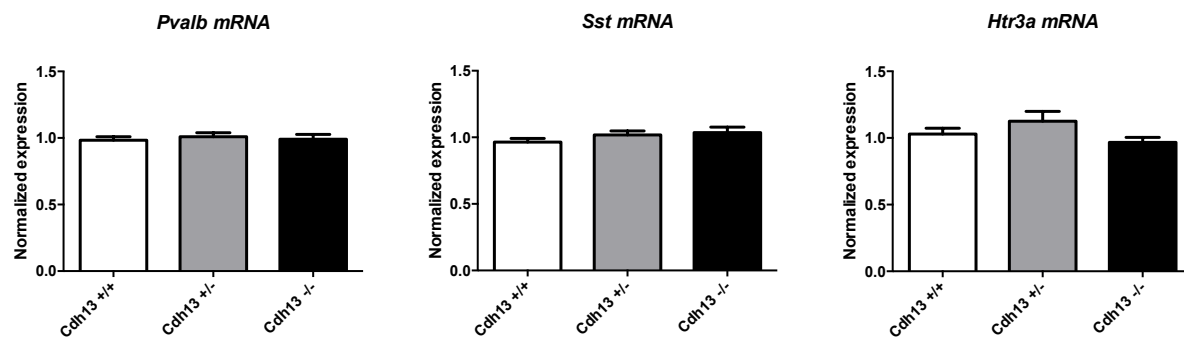
Figure 30: Normalized expression of the interneuron marker *Pvalb, Sst* and *Htr3a* in the hippocampus. The bars represent mean normalized expression. Error bars represent SEM. Kruskal-Wallis test revealed no significant differences between genotypes. (n=10-12 per genotype)

3.2.2. Effects on the glutamatergic system

Glutamate transporter

The normalized expression of vesicular glutamate transporter mRNA was similar among genotypes for all three isoforms. Again, the differences reached no significant threshold. Also notable are the relatively high SEM values in *Vglut2* compared to other samples.
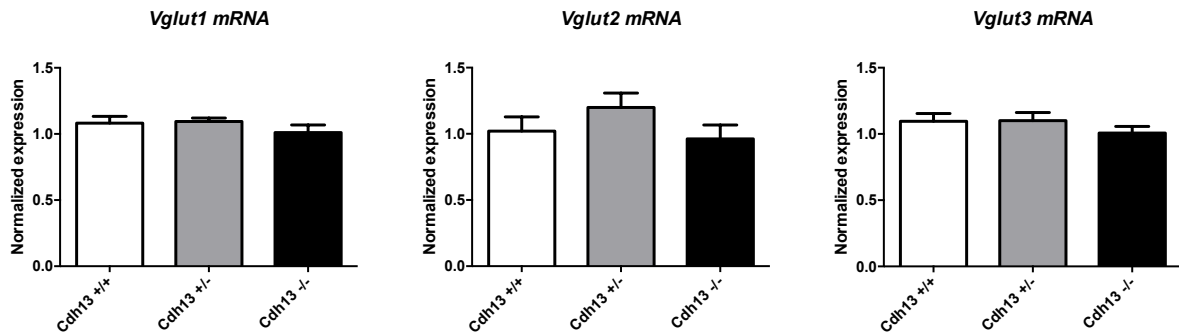
Figure 31: Normalized expression of the vesicular glutamate transporter *Vglut1*, *Vglut2*, *Vglut3* in the hippocampus. The bars represent mean normalized expression. Error bars represent SEM. Kruskal-Wallis test revealed no significant differences between genotypes. (n=10-12 per genotype)

Postsynaptic membrane proteins

The analysis of Post-Synaptic Density Protein 95, a scaffold protein found in the postsynaptic membrane of excitatory glutamatergic synapses, revealed no statistical significant differences among genotypes (Figure 32).

Figure 32: Normalized expression of postsynaptic scaffold protein *Psd95* in the hippocampus. The bars represent mean normalized expression. Error bars represent SEM. Kruskal-Wallis test revealed no significant differences between genotypes. (n=10-12 per genotype)

4. Discussion

In this thesis, the influence of CDH13 deficiency on the population of GABAergic interneurons in the stratum oriens of the hippocampus was investigated.
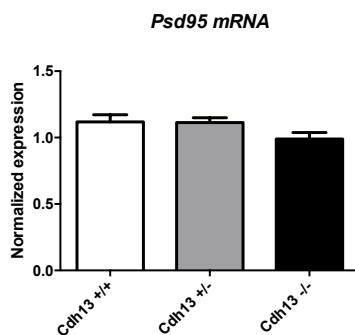
CDH13 is an atypical member of the cadherin superfamily of type-1 transmembrane cellular adhesion proteins. It is widely distributed in the brain and shows a high cellular expression in hippocampal interneurons, especially in the group of PV- and SOM-positive cells, while nNOS-positive cells show a low degree of colocalization (Rivero, Selten et al. 2015). The low adhesiveness and structural differences of CDH13 compared to classical cadherins makes it likely that it also serves as a neuronal receptor and signaling molecule. Members of the cadherin superfamily are known to regulate neuronal development and axon guidance in various parts of the brain. CDH13 was found to act as regulator for axon outgrowth in motor neurons and GABAergic and glutamatergic synaptogenesis in hippocampal dissociated neurons (Paradis, Harrar et al. 2007, Ciatto, Bahna et al. 2010, Fiederling, Ewert et al. 2011, Najarro, Wong et al. 2012, Rivero, Selten et al. 2015).

Thus, we hypothesized that CDH13 deficiency has an impact on hippocampal interneurons and their neurotransmission, not least because of various studies that linked interneuron dysfunction to psychiatric disorders (Ramamoorthi and Lin 2011, Marin 2012).

4.1 *Cdh13* knockout mice have a reduced gene expression of *TrkB* in the hippocampus

Notably, we found significant differences among genotypes in the expression of tropomyosin-related kinase B (*TrkB*) mRNA (p = 0.0156 in the Kruskal-Wallis test). Tukey's multiple comparisons test revealed that *TrkB* is lower expressed in *Cdh13*$^{-/-}$ mice compared to wildtype (adjusted P = 0.0075) and heterozygote animals (adjusted P = 0.0148).

TrkB is a neutrophin receptor that is widely distributed within the central nervous system. In the adult hippocampus it is strongly expressed in glutamatergic pyramidal and granule cells, but also occasionally in interneurons (Drake, Milner et al. 1999). Although the receptor and its ligand BDNF are best known for their role in survival and differentiation of neuronal cells (Lu and Gottschalk 2000), they also play a major role in synaptic plasticity and particularly in long-term potentiation (LTP), the most important correlate of memory formation in the brain (Chao 2003, Cooke and Bliss 2006). Mice lacking BDNF have reduced rates of successful early-phase LTP inductions in the hippocampal CA1 area, while hippocampal tissue blocked with TrkB antibodies shows impairments in late-phase LTP (Korte, Carroll et al. 1995, Korte,

Kang et al. 1998, Minichiello 2009), suggesting that TrkB and BDNF act as key regulators in different stages of LTP induction and maintenance (Minichiello 2009). Consequently, TrkB also impacts learning behavior. Mice with a conditional *TrkB* knockout limited to the forebrain that only occurs during the postnatal development phase show strong spatial learning and memory impairment in the Morris Water Maze (Minichiello, Korte et al. 1999). Interestingly, decreased *TrkB* mRNA levels were found in the prefrontal cortex (PFC) of human schizophrenia subjects that correlated with altered GABA-related gene expression (Hashimoto, Bergen et al. 2005). The same authors used *TrkB*-hypomorphic mice (Xu, Gottschalk et al. 2000) to show that genetically introduced decreases in TrkB expression result in reduced *GAD1* and *PV* mRNA levels in the PFC. These findings suggest that altered TrkB signaling causes dysfunctions of (particularly PV-positive) interneurons (Hashimoto, Bergen et al. 2005), which in turn could disrupt the function of inhibitory circuits (Ramamoorthi and Lin 2011, Nakazawa, Zsiros et al. 2012). As mentioned before, excitatory–inhibitory imbalances are believed to contribute to clinical features of several neurodevelopmental disorders (Marin 2012).

There are three major signaling pathways that can be activated by the TrkB receptor: the PI3K/Akt/GSK3 pathway, the Ras/MAPK pathway and the PLC γ /Ca2+ pathway (Minichiello 2009). Downstream of PI3K and Akt, several effectors control neurite outgrowth, synaptogenesis and synaptic transmission (Read and Gorman 2009, Rivero, Sich et al. 2013). Mice treated with PI3K inhibitor wortmannin also show impaired spatial learning, suggesting that the pathway plays a role in BDNF-dependent memory formation (Mizuno, Yamada et al. 2003, Yamada and Nabeshima 2003). Notably, CDH13 was found to affect the PI3K/Akt/GSK3 pathway in vascular endothelial cells via its physical interaction with the scaffold protein integrin-linked kinase (Joshi, Ivanov et al. 2007, Rivero, Sich et al. 2013). As CDH13 lacks the typical transmembrane and cytoplasmatic domain, it requires other molecules to ensure the onward transmission of the signal to the cytoplasm of the target cell (Rivero, Sich et al. 2013). Homophilic and heterophilic cadherin interactions were found to regulate different pathways involved in cellular polarization, adhesion and migration, particularly in vascular endothelial cells (Ivanov, Philippova et al. 2004, Philippova, Ivanov et al. 2005, Philippova, Joshi et al. 2009). In the brain, CDH13 may interact with receptor tyrosine kinases (RTKs) such as TrkB to activate the PI3K/Akt/GSK3 pathway, as interactions of cell adhesion molecules with RTKs have been described before (Rivero, Sich et al. 2013). Several findings suggest that cadherins can regulate the activity of RTKs directly

(Wheelock and Johnson 2003). Pece and Gutkind (2000) showed that E-cadherin is able to stimulate the Ras/MAPK pathway via ligand-independent activation of the epidermal growth factor receptor.

Therefore, CDH13 could be considered as an interaction partner of TrkB in the brain. Given the fact that the expression level of TrkB, which plays a major role in neurite outgrowth, synaptic plasticity, LTP and memory formation is reduced in *Cdh13* knockout mice, one might assume that CDH13 acts as a regulator of TrkB and its downstream pathways. This finding draws a functional link to work from our laboratory, which showed increased learning deficits and cognitive inflexibility in *Cdh13* knockout mice (Rivero, Selten et al. 2015).

The exact mechanism how CDH13 deficiency reduces the expression of *TrkB* mRNA remains elusive. The gene transcription of *TrkB* was found to be highly activity-dependent. Depolarization of cultured mouse cortical neurons increases the expression of full-length TrkB transcripts and protein (West, Griffith et al. 2002, Kingsbury, Murray et al. 2003, Lei and Parada 2007). Therefore, it could be hypothesized that the reduced gene expression of TrkB in CDH13 deficient mice is a result of decreased hippocampal activity.

In the hippocampus, TrkB is mainly expressed in pyramidal cells (Drake, Milner et al. 1999). In *Cdh13* knockout mice, these neurons were found to receive higher inhibitory inputs in the CA1 area (Rivero, Selten et al. 2015), which would likely provoke excitatory–inhibitory imbalances. One could assume that the increased inhibitory inputs result in a reduced TrkB transcription rate. Although this might be a promising explanatory approach for the CDH13/TrkB interaction, further research is necessary, especially to determine if protein levels and phosphorylation of TrkB are also affected.

Contrary to our expectations, the expression of no other tested gene was significantly influenced by the deficiency of CDH13. It could be possible that CDH13 deficiency causes changes in the protein activity as several proteins, including Akt, can be regulated by phosphorylation, which leaves the mRNA level unaltered (Hassan, Akcakanat et al. 2013). Another possibility might be that CDH13-associated hippocampal dysfunctions are dependent on environmental factors. Therefore, gene expression analysis of mice with different early life experiences could be an interesting approach.

Although the gene expression of *TrkB*, which plays an important role in GABAergic interneuron development, maturation and survival (Alcantara, Frisen et al. 1997, Huang,

Kirkwood et al. 1999, Yamada, Nakanishi et al. 2002), is reduced in *Cdh13* knockout mice, GABA-related gene expression shows now alterations in the whole hippocampus. One might hypothesize that the decrease of TrkB is too small to cause measurable differences in the expression of GABA-related genes or that different regions of the hippocampus show different results in that regard.

The GABA-A receptor α1 subunit has been shown to be directly associated with CDH13 in lipid rafts of vascular endothelial cells (Philippova, Ivanov et al. 2008). As it is also expressed in PV-positive interneurons, the missing effect of CDH13 deficiency on the receptor expression in the hippocampus suggests a different role in neuronal cells.

Researchers have identified several other signaling adaptors of CDH13. This includes GRP78, a molecular chaperone in the endoplasmic reticulum (ER) (Philippova, Ivanov et al. 2008). These findings are of particular importance as GRP78 can be linked to CDH13 dependent cell survival. Many other molecules, such as integrins and growth factor receptors, are believed to be involved in CDH13-dependent signal transduction in neuronal pathways (Rivero, Sich et al. 2013). Neuronal integrins are mediating neurite outgrowth via their attachment to the extracellular matrix. Growth factor receptors have been found to take part in the formation of neural circuits through their interaction with other neuronal cell adhesion molecules such as DCAM, making these molecules a promising approach for further CDH13 research (Hansen, Berezin et al. 2008, Rivero, Sich et al. 2013).

4.2 *Cdh13* knockout mice show no alterations in different inhibitory interneuron populations

Contrary to our expectations, CDH13 deficiency did not significantly influence the quantity or density of different inhibitory interneuron populations, neither the size of the SO. The insignificant results of the analysis of the nNOS-stained brains are not surprising, as nNOS-expressing interneurons have a low degree of colocalization with CDH13, therefore an effect of CDH13 deficience in this population is not expected. While the volume of the complete SO among different genotypes appears to be quite homogenous, there are greater discrepancies in the subdivision into ventral and dorsal hippocampus. In PV-stained brains the subdivisions have almost the same size. In SOM- and nNOS-stained brains the ventral part is slightly smaller, yet there is wide variance among genotypes in the nNOS-stained brains. One possible explanation is the division of the whole hippocampus into 6 series per brain, which might have led to unrepresentative distributions of ventral and dorsal hippocampus sections.

Of particular importance in this context is the clear difference of cell quantity and density between the ventral and dorsal hippocampus. PV and SOM-stained brains have largely increased cell populations and densities in the ventral hippocampus compared to the dorsal hippocampus. These findings concord largely with results from a quantitative analysis of chemically defined hippocampal interneurons by Jinno and Kosaka (2006). The authors found nNOS-expressing cells to be denser in the dorsal hippocampus in CA1 and in the ventral hippocampus in CA3, which might explain the balanced density results we found in our study, which did not distinguish between different CA sections.

Given the results of the colocalization study described earlier, it can be assumed that CDH13-positive interneurons in the hippocampus might be axo-axonic cells (expressing PV), basket cells (expressing PV), bistratified cells (expressing PV and SOM) or O-LM cells (expressing PV and SOM) (Somogyi and Klausberger 2005). For a more detailed distinction, morphological and electrophysiological properties would be required.

Although alterations in the hippocampal interneuron population could not be found in this study, there is considerable evidence that CDH13 plays a crucial role in the establishment and maintenance of neural circuits, both in the hippocampus and other parts of the brain. The formation of neural circuits is a complex process that depends both on extracellular cues and intracellular signal transduction resulting in cytoskeletal changes (Hansen, Berezin et al. 2008).

Hayano, Zhao et al. (2014) showed that CDH13 is involved in the formation of axonal pathways in the neocortex of the developing rat brain. Most recently, Killen, Barber et al. (2017) found CDH13 to have a protective role in cortical interneuron development. They showed that developing *Cdh13* knockout mice have reduced numbers of interneurons and pyramidal neurons in the cortex at the stage E18.5, presumably caused by increased apoptosis. This assumption is backed by other studies that emphasize the role of CDH13 as regulator of cell-survival, among others in vascular and melanoma cells (Philippova, Ivanov et al. 2008, Bosserhoff, Ellmann et al. 2014). The findings from Killen et al. are somewhat surprising, given the fact that we could not find any neuron number alterations in the adult hippocampus, which shows the highest cellular CDH13 expression. One might therefore conclude that these quantitative differences among genotypes only occur during a late stage of development and are somehow compensated afterwards. Thus, more detailed investigations of the developing hippocampus should be subject of future research. Another explanation would be methodological differences. Killen and colleagues counted within "a 300 μ m segment [that]

was measured along the ventricular surface of the cortex next to the cortico-striatal junction", while we used the whole *stratum oriens* of the hippocampus. Unlike our division into different interneuron subclasses, they simply used a GAD67 staining to identify interneurons. Finally, they used 5 brains per genotype and only analyzed $Cdh13^{+/+}$ and $Cdh13^{-/-}$ mice, while we used 7-9 brains per genotypes and also included heterozygotes.

Even though interneuron alterations could not be found in the SO of the adult murine hippocampus, electrophysiological testing unveiled that neurons from $Cdh13$ knockout mice have higher inhibitory inputs in the CA1 area (Rivero, Selten et al. 2015). Taking into consideration that there were no detectable differences in the expression of genes involved GABAergic neurotransmission in the mice analyzed in the present study, it would be interesting to know if the pyramidal cells are affected by CDH13 deficiency. A lower number of those neurons with a consistent GABAergic transmission might explain a higher individual input reaching those cells. Another possibility would be altered synaptic connections resulting from $Cdh13$ inactivation, which result in higher inputs in those CA1 cells, while other cells received lower inputs. This finding suggests that CDH13 acts as crucial mediator for the delicate balance between inhibitory and excitatory inputs in the hippocampus (Rivero, Selten et al. 2015), although many questions remain open for future research.

As mentioned before, alterations in the susceptible inhibitory circuits of the hippocampus have been linked to mental disorders several times (Marin 2012). Interestingly, other genes involved in synaptic plasticity of hippocampal PV-positive interneurons such as $ErbB4$ have also been linked to psychiatric disorders (Vullhorst, Neddens et al. 2009, Ramamoorthi and Lin 2011, Rivero, Selten et al. 2015). Furthermore, dysfunction of PV-positive interneurons and resulting alterations in the GABAergic system were found to trigger schizophrenia-like symptoms, particularly in the PFC (Hashimoto, Bergen et al. 2005, Nakazawa, Zsiros et al. 2012). Other neurodevelopmental disorders are heavily influenced by inhibitory interneurons, as well. Fernandez, Morishita et al. (2007) showed that pharmacological modulation of the GABAergic system via GABA A receptor antagonists could be a promising strategy in patients with Down syndrome.

Although mostly limited to mouse models, all these findings emphasize the role of the inhibitory GABAergic system and particularly PV-positive interneurons in the pathogenesis of neurodevelopmental disorders such as ADHD. Even though association studies with genome-wide significance for $CDH13$ are still outstanding, there is strong evidence of the involvement of $CDH13$ in the etiology of this common neurodevelopmental disorder. Work

from our laboratory showed increased learning deficits and cognitive inflexibility in *Cdh13* knockout mice, a finding that shows remarkable similarities to ADHD patients (Rivero, Selten et al. 2015). The same study showed that *Cdh13* knockout mice had increased locomotor activity, which represents a cardinal symptom of ADHD.

4.3 Final remarks

In this context, it should be pointed out that the important role of CDH13 in the brain is not limited to the GABAergic system. CDH13 was found to be crucial in the development of the serotonergic system in the dorsal raphe (Forero, Rivero et al. 2017) and alterations in this system have been linked to the pathogenesis of neurodevelopmental disorders several times (Lesch and Waider 2012).

Taken together, the results of this thesis indicate that there is no direct influence of CDH13 deficiency on the quantity of GABAergic interneurons in the SO of adult mice. In contrast, CDH13 deficiency significantly decreases the expression of TrkB, a receptor of the neurotrophic factor BDNF in the hippocampus. Furthermore, results from other studies leave no doubt that CDH13 has a lasting effect on the GABAergic system, both in the hippocampus and in other cortical areas. Many findings also emphasize the role of CDH13 as a risk factor for ADHD and other neurodevelopmental disorders. This includes work from our laboratory that showed ADHD-like behavior in *Cdh13* knockout mice.

Summarizing the above, it can be said that there are many evident links between CDH13, the hippocampal GABAergic system and ADHD, although the complex interactions that contribute to the pathophysiology have to be further investigated.

4.4 Limitations of the study

In the stereology study, possible sources of error occurred during the sectioning and staining of the hippocampus. In some cases, it was rather difficult to adjust the axis of the brain in the cryostat, leading to oblique orientation in a part of the samples and therefore inconsistent classification into anterior and posterior hippocampus. Therefore, a subdivision into CA1, CA2 and CA3 might have been a better approach, especially because the neuron populations vary considerably among the different regions. Also, some samples were partially damaged during the staining process. Yet, the very homogenous results of the volume analysis, particularly of the PV-expressing neurons, suggest that this did not influence the results.

Another limitation is the classification of the heterogeneous interneuron subpopulations with chemical markers. As shown in Figure 9, PV and SOM had the highest levels of coexpression, but did not reach percentage values over ~50 %. This could be caused by the fact that markers are expressed in more than one cell type and show a certain level of overlapping (Figure 4). If we assume that only some populations of interneurons are affected by CDH13 and that the genotype effect size is relatively small, an interference of the subgroups might disguise a possible effect of the deficiency. Consequently, better criteria for interneuron characterization, cell-specific *Cdh13* knockout and larger sample sizes would be desirable.

In the qRT-PCR study, problems occurred during the sectioning of the brains on a cold plate. The high room temperatures in the summer caused those brain sections that did not have direct contact to the plate to partially melt. The conducted quality controls did not indicate any changes in the RNA integrity of those samples though. Other possible sources of error occurred with the thermal cycler. Several samples showed a low efficiency in the subsequent analysis, probably caused by improper calibration. To make sure possible effects of the deficiency are not overlooked, qRT-PCR was repeated for several affected genes with identical results to the initial experiments.

5. Annex

5.1 Supplementary Tables

Sample ID	Concentration in ng/ul	Absorbance at 260 nm	Absorbance at 280 nm	260/280 ratio
1	488.96	12.224	5.765	2.12
2	275.17	6.879	3.304	2.08
3	291.87	7.297	3.475	2.1
4	348.74	8.718	4.226	2.06
6	295.92	7.398	3.568	2.07
7	481.06	12.027	5.683	2.12
10	303.48	7.587	3.618	2.1
11	391.33	9.783	4.716	2.07
12	303.29	7.582	3.639	2.08
13	318.68	7.967	3.822	2.08
17	290.64	7.266	3.468	2.1
18	238.23	5.956	2.823	2.11
19	314.78	7.87	3.746	2.1
20	367.8	9.195	4.484	2.05
21	380.63	9.516	4.613	2.1
22	352.07	8.802	4.211	2.09
23	213.42	5.335	2.561	2.08
24	307.33	7.683	3.698	2.08
26	210.13	5.253	2.507	2.1
28	401.86	10.047	4.894	2.05
31	318.02	7.951	3.856	2.06
38	265.56	6.639	3.207	2.07
39	277.67	6.942	3.289	2.11
46	433.91	10.848	5.368	2.02
47	247.44	6.186	2.963	2.09
48	280.91	7.023	3.336	2.11
56	306.82	7.67	3.683	2.08
63	271.08	6.777	3.274	2.07
64	195.88	4.897	2.319	2.11
65	315.29	7.882	3.813	2.07
67	481.43	12.036	5.938	2.03
88	373.7	9.343	4.549	2.05
89	427.83	10.696	5.212	2.05
90	260.45	6.511	3.099	2.1
95	295.55	7.389	3.554	2.08

Supplementary Table 1: Results of the NanoDrop analysis of RNA samples including concentration and absorbance maxima. All samples reached the expected 260/280 ratio of ~2.0, indicating highly pure RNA (Desjardins and Conklin 2010).

5.2 References

Abercrombie, M. (1946). "Estimation of nuclear population from microtome sections." Anat Rec **94**: 239-247.

Aika, Y., J. Q. Ren, K. Kosaka and T. Kosaka (1994). "Quantitative analysis of GABA-like-immunoreactive and parvalbumin-containing neurons in the CA1 region of the rat hippocampus using a stereological method, the disector." Experimental Brain Research **99**(2): 267-276.

Alcantara, S., J. Frisen, J. A. del Rio, E. Soriano, M. Barbacid and I. Silos-Santiago (1997). "TrkB signaling is required for postnatal survival of CNS neurons and protects hippocampal and motor neurons from axotomy-induced cell death." J Neurosci **17**(10): 3623-3633.

Amaral, D. G., H. E. Scharfman and P. Lavenex (2007). "The dentate gyrus: fundamental neuroanatomical organization (dentate gyrus for dummies)." Prog Brain Res **163**: 3-22.

American Psychiatric Association (2013). Attention-Deficit/Hyperactivity Disorder. Diagnostic and Statistical Manual of Mental Disorders. Washington, DC.

Andersen, P. (2007). The hippocampus book. Oxford [u.a.], Oxford Univ. Press.

Andersen, P., T. V. P. Bliss and K. K. Skrede (1971). "Lamellar organization of hippocampal excitatory pathways." Experimental Brain Research **13**(2): 222-238.

Angst, B. D., C. Marcozzi and A. I. Magee (2001). "The cadherin superfamily: diversity in form and function." J Cell Sci **114**(Pt 4): 629-641.

Ascoli, G. A., L. Alonso-Nanclares, S. A. Anderson, G. Barrionuevo, R. Benavides-Piccione, A. Burkhalter, G. Buzsaki, B. Cauli, J. Defelipe, A. Fairen, D. Feldmeyer, G. Fishell, Y. Fregnac, T. F. Freund, D. Gardner, E. P. Gardner, J. H. Goldberg, M. Helmstaedter, S. Hestrin, F. Karube, Z. F. Kisvarday, B. Lambolez, D. A. Lewis, O. Marin, H. Markram, A. Munoz, A. Packer, C. C. Petersen, K. S. Rockland, J. Rossier, B. Rudy, P. Somogyi, J. F. Staiger, G. Tamas, A. M. Thomson, M. Toledo-Rodriguez, Y. Wang, D. C. West and R. Yuste (2008). "Petilla terminology: nomenclature of features of GABAergic interneurons of the cerebral cortex." Nat Rev Neurosci **9**(7): 557-568.

Banaschewski, T., K. Becker, M. Dopfner, M. Holtmann, M. Rosler and M. Romanos (2017). "Attention-Deficit/Hyperactivity Disorder." Dtsch Arztebl Int **114**(9): 149-159.

Banaschewski, T., K. Becker, S. Scherag, B. Franke and D. Coghill (2010). "Molecular genetics of attention-deficit/hyperactivity disorder: an overview." European Child & Adolescent Psychiatry **19**(3): 237-257.

Batista-Brito, R., R. Machold, C. Klein and G. Fishell (2008). "Gene expression in cortical interneuron precursors is prescient of their mature function." Cereb Cortex **18**(10): 2306-2317.

Beaulieu, J. M. (2012). "A role for Akt and glycogen synthase kinase-3 as integrators of dopamine and serotonin neurotransmission in mental health." J Psychiatry Neurosci **37**(1): 7-16.

Berx, G. and F. Van Roy (2001). "The E-cadherin/catenin complex: an important gatekeeper in breast cancer tumorigenesis and malignant progression." Breast Cancer Res **3**(5): 289-293.

Bettler, B., K. Kaupmann, J. Mosbacher and M. Gassmann (2004). "Molecular structure and physiological functions of GABA(B) receptors." Physiol Rev **84**(3): 835-867.

Bezaire, M. J. and I. Soltesz (2013). "Quantitative assessment of CA1 local circuits: knowledge base for interneuron-pyramidal cell connectivity." Hippocampus **23**(9): 751-785.

Bird, C. M. and N. Burgess (2008). "The hippocampus and memory: insights from spatial processing." Nat Rev Neurosci **9**(3): 182-194.

Bonvicini, C., S. V. Faraone and C. Scassellati (2016). "Attention-deficit hyperactivity disorder in adults: A systematic review and meta-analysis of genetic, pharmacogenetic and biochemical studies." Mol Psychiatry **21**(7): 872-884.

Bosserhoff, A. K., L. Ellmann, A. S. Quast, J. Eberle, G. M. Boyle and S. Kuphal (2014). "Loss of T-cadherin (CDH-13) regulates AKT signaling and desensitizes cells to apoptosis in melanoma." Molecular Carcinogenesis **53**(8): 635-647.

Chao, M. V. (2003). "Neurotrophins and their receptors: a convergence point for many signalling pathways." Nat Rev Neurosci **4**(4): 299-309.

Christofori, G. and H. Semb (1999). "The role of the cell-adhesion molecule E-cadherin as a tumour-suppressor gene." Trends Biochem Sci **24**(2): 73-76.

Ciatto, C., F. Bahna, N. Zampieri, H. C. VanSteenhouse, P. S. Katsamba, G. Ahlsen, O. J. Harrison, J. Brasch, X. Jin, S. Posy, J. Vendome, B. Ranscht, T. M. Jessell, B. Honig and L. Shapiro (2010). "T-cadherin structures reveal a novel adhesive binding mechanism." Nat Struct Mol Biol **17**(3): 339-347.

Cohen, N. J. and L. R. Squire (1980). "Preserved learning and retention of pattern-analyzing skill in amnesia: dissociation of knowing how and knowing that." Science **210**(4466): 207-210.

Colonnier, M. L. (1965). The Structural Design of the Neocortex. Brain and Conscious Experience: Study Week September 28 to October 4, 1964, of the Pontificia Academia Scientiarum. J. C. Eccles. Berlin, Heidelberg, Springer Berlin Heidelberg**:** 1-23.

Contreras, D. (2004). "Electrophysiological classes of neocortical neurons." Neural Networks **17**(5): 633-646.

Cooke, S. F. and T. V. P. Bliss (2006). "Plasticity in the human central nervous system." Brain **129**(7): 1659-1673.

Couve, A., S. J. Moss and M. N. Pangalos (2000). "GABAB receptors: a new paradigm in G protein signaling." Mol Cell Neurosci **16**(4): 296-312.

Cuffe, S. P., C. G. Moore and R. E. McKeown (2005). "Prevalence and correlates of ADHD symptoms in the national health interview survey." J Atten Disord **9**(2): 392-401.

Dames, S. A., E. Bang, D. Haussinger, T. Ahrens, J. Engel and S. Grzesiek (2008). "Insights into the low adhesive capacity of human T-cadherin from the NMR structure of Its N-terminal extracellular domain." J Biol Chem **283**(34): 23485-23495.

Derycke, L. D. and M. E. Bracke (2004). "N-cadherin in the spotlight of cell-cell adhesion, differentiation, embryogenesis, invasion and signalling." Int J Dev Biol **48**(5-6): 463-476.

Desjardins, P. and D. Conklin (2010). "NanoDrop Microvolume Quantitation of Nucleic Acids." J Vis Exp(45).

Ding, S. L. (2013). "Comparative anatomy of the prosubiculum, subiculum, presubiculum, postsubiculum, and parasubiculum in human, monkey, and rodent." J Comp Neurol **521**(18): 4145-4162.

Drake, C. T., T. A. Milner and S. L. Patterson (1999). "Ultrastructural localization of full-length trkB immunoreactivity in rat hippocampus suggests multiple roles in modulating activity-dependent synaptic plasticity." J Neurosci **19**(18): 8009-8026.

Eller, J., S. Zarnadze, P. Bäuerle, T. Dugladze and T. Gloveli (2015). "Cell Type-Specific Separation of Subicular Principal Neurons during Network Activities." PLoS One **10**(4).

Emamian, E. S., D. Hall, M. J. Birnbaum, M. Karayiorgou and J. A. Gogos (2004). "Convergent evidence for impaired AKT1-GSK3beta signaling in schizophrenia." Nat Genet **36**(2): 131-137.

Faraone, S. V., J. Biederman and E. Mick (2006). "The age-dependent decline of attention deficit hyperactivity disorder: a meta-analysis of follow-up studies." Psychol Med **36**(2): 159-165.

Faraone, S. V., A. E. Doyle, J. Lasky-Su, P. B. Sklar, E. D'Angelo, J. Gonzalez-Heydrich, C. Kratochvil, E. Mick, K. Klein, A. J. Rezac and J. Biederman (2008). "Linkage Analysis of Attention Deficit Hyperactivity Disorder." Am J Med Genet B Neuropsychiatr Genet **0**(8): 1387-1391.

Faraone, S. V., R. H. Perlis, A. E. Doyle, J. W. Smoller, J. J. Goralnick, M. A. Holmgren and P. Sklar (2005). "Molecular genetics of attention-deficit/hyperactivity disorder." Biol Psychiatry **57**(11): 1313-1323.

Fernandez, F., W. Morishita, E. Zuniga, J. Nguyen, M. Blank, R. C. Malenka and C. C. Garner (2007). "Pharmacotherapy for cognitive impairment in a mouse model of Down syndrome." Nat Neurosci **10**(4): 411-413.

Fiederling, A., R. Ewert, A. Andreyeva, K. Jungling and K. Gottmann (2011). "E-cadherin is required at GABAergic synapses in cultured cortical neurons." Neurosci Lett **501**(3): 167-172.

Ford, T., R. Goodman and H. Meltzer (2003). "The British Child and Adolescent Mental Health Survey 1999: the prevalence of DSM-IV disorders." J Am Acad Child Adolesc Psychiatry **42**(10): 1203-1211.

Forero, A., O. Rivero, S. Waldchen, H. P. Ku, D. P. Kiser, Y. Gartner, L. S. Pennington, J. Waider, P. Gaspar, C. Jansch, F. Edenhofer, T. J. Resink, R. Blum, M. Sauer and K. P. Lesch (2017). "Cadherin-13 Deficiency Increases Dorsal Raphe 5-HT Neuron Density and Prefrontal Cortex Innervation in the Mouse Brain." Front Cell Neurosci **11**: 307.

Franke, B., S. V. Faraone, P. Asherson, J. Buitelaar, C. H. Bau, J. A. Ramos-Quiroga, E. Mick, E. H. Grevet, S. Johansson, J. Haavik, K. P. Lesch, B. Cormand and A. Reif (2012). "The genetics of attention deficit/hyperactivity disorder in adults, a review." Mol Psychiatry **17**(10): 960-987.

Franke, B., B. M. Neale and S. V. Faraone (2009). "Genome-wide association studies in ADHD." Human Genetics **126**(1): 13-50.

Fredette, B. J., J. Miller and B. Ranscht (1996). "Inhibition of motor axon growth by T-cadherin substrata." Development **122**(10): 3163-3171.

Fredette, B. J. and B. Ranscht (1994). "T-cadherin expression delineates specific regions of the developing motor axon-hindlimb projection pathway." J Neurosci **14**(12): 7331-7346.

Freund, T. F. and G. Buzsaki (1996). "Interneurons of the hippocampus." Hippocampus **6**(4): 347-470.

Fyhn, M., S. Molden, M. P. Witter, E. I. Moser and M.-B. Moser (2004). "Spatial Representation in the Entorhinal Cortex." Science **305**(5688): 1258-1264.

Galanopoulou, A. S. (2010). "Mutations affecting GABAergic signaling in seizures and epilepsy." Pflugers Arch **460**(2): 505-523.

Gulyas, A. I., N. Hajos, I. Katona and T. F. Freund (2003). "Interneurons are the local targets of hippocampal inhibitory cells which project to the medial septum." Eur J Neurosci **17**(9): 1861-1872.

Gundersen, H. J., P. Bagger, T. F. Bendtsen, S. M. Evans, L. Korbo, N. Marcussen, A. Moller, K. Nielsen, J. R. Nyengaard, B. Pakkenberg and et al. (1988). "The new stereological tools: disector, fractionator, nucleator and point sampled intercepts and their use in pathological research and diagnosis." Apmis **96**(10): 857-881.

Gundersen, H. J., T. F. Bendtsen, L. Korbo, N. Marcussen, A. Moller, K. Nielsen, J. R. Nyengaard, B. Pakkenberg, F. B. Sorensen, A. Vesterby and et al. (1988). "Some new, simple and efficient stereological methods and their use in pathological research and diagnosis." Apmis **96**(5): 379-394.

Halbleib, J. M. and W. J. Nelson (2006). "Cadherins in development: cell adhesion, sorting, and tissue morphogenesis." Genes Dev **20**(23): 3199-3214.

Hansen, S. M., V. Berezin and E. Bock (2008). "Signaling mechanisms of neurite outgrowth induced by the cell adhesion molecules NCAM and N-cadherin." Cell Mol Life Sci **65**(23): 3809-3821.

Hashimoto, T., S. E. Bergen, Q. L. Nguyen, B. Xu, L. M. Monteggia, J. N. Pierri, Z. Sun, A. R. Sampson and D. A. Lewis (2005). "Relationship of brain-derived neurotrophic factor and

its receptor TrkB to altered inhibitory prefrontal circuitry in schizophrenia." Journal of Neuroscience **25**(2): 372-383.

Hassan, B., A. Akcakanat, A. M. Holder and F. Meric-Bernstam (2013). "Targeting the PI3-kinase/Akt/mTOR signaling pathway." Surg Oncol Clin N Am **22**(4): 641-664.

Hayano, Y., H. Zhao, H. Kobayashi, K. Takeuchi, S. Norioka and N. Yamamoto (2014). "The role of T-cadherin in axonal pathway formation in neocortical circuits." Development **141**(24): 4784-4793.

Hermey, G. (2011). Der Experimentator: Neurowissenschaften. Experimentator. Heidelberg, Spektrum Akademischer Verlag.

Huang, Z. J., A. Kirkwood, T. Pizzorusso, V. Porciatti, B. Morales, M. F. Bear, L. Maffei and S. Tonegawa (1999). "BDNF regulates the maturation of inhibition and the critical period of plasticity in mouse visual cortex." Cell **98**(6): 739-755.

Ishizuka, N., W. M. Cowan and D. G. Amaral (1995). "A quantitative analysis of the dendritic organization of pyramidal cells in the rat hippocampus." J Comp Neurol **362**(1): 17-45.

Ivanov, D., M. Philippova, V. Tkachuk, P. Erne and T. Resink (2004). "Cell adhesion molecule T-cadherin regulates vascular cell adhesion, phenotype and motility." Exp Cell Res **293**(2): 207-218.

Jacob, T. C., S. J. Moss and R. Jurd (2008). "GABAA receptor trafficking and its role in the dynamic modulation of neuronal inhibition." Nature Reviews Neuroscience **9**: 331.

Jensen, C. M. and H. C. Steinhausen (2015). "Comorbid mental disorders in children and adolescents with attention-deficit/hyperactivity disorder in a large nationwide study." Atten Defic Hyperact Disord **7**(1): 27-38.

Jinno, S. and T. Kosaka (2006). "Cellular architecture of the mouse hippocampus: a quantitative aspect of chemically defined GABAergic neurons with stereology." Neurosci Res **56**(3): 229-245.

Jonas, P. and J. Lisman (2014). "Structure, function, and plasticity of hippocampal dentate gyrus microcircuits." Front Neural Circuits **8**.

Jones, A. R., C. C. Overly and S. M. Sunkin (2009). "The Allen Brain Atlas: 5 years and beyond." Nat Rev Neurosci **10**(11): 821-828.

Joseph N. Pierri, Adil S. Chaudry, Tsung-Ung W. Woo and David A. Lewis (1999). "Alterations in Chandelier Neuron Axon Terminals in the Prefrontal Cortex of Schizophrenic Subjects." American Journal of Psychiatry **156**(11): 1709-1719.

Joshi, M. B., D. Ivanov, M. Philippova, P. Erne and T. J. Resink (2007). "Integrin-linked kinase is an essential mediator for T-cadherin-dependent signaling via Akt and GSK3beta in endothelial cells." Faseb j **21**(12): 3083-3095.

Killen, A. C., M. Barber, J. J. W. Paulin, B. Ranscht, J. G. Parnavelas and W. D. Andrews (2017). "Protective role of Cadherin 13 in interneuron development." Brain Structure and Function.

Kingsbury, T. J., P. D. Murray, L. L. Bambrick and B. K. Krueger (2003). "Ca(2+)-dependent regulation of TrkB expression in neurons." J Biol Chem **278**(42): 40744-40748.

Klausberger, T. (2009). "GABAergic interneurons targeting dendrites of pyramidal cells in the CA1 area of the hippocampus." Eur J Neurosci **30**(6): 947-957.

Klausberger, T. and P. Somogyi (2008). "Neuronal diversity and temporal dynamics: the unity of hippocampal circuit operations." Science **321**(5885): 53-57.

Korte, M., P. Carroll, E. Wolf, G. Brem, H. Thoenen and T. Bonhoeffer (1995). "Hippocampal long-term potentiation is impaired in mice lacking brain-derived neurotrophic factor." Proceedings of the National Academy of Sciences **92**(19): 8856-8860.

Korte, M., H. Kang, T. Bonhoeffer and E. Schuman (1998). "A role for BDNF in the late-phase of hippocampal long-term potentiation." Neuropharmacology **37**(4-5): 553-559.

Kwon, J. M. and A. M. Goate (2000). "The candidate gene approach." <u>Alcohol Res Health</u> **24**(3): 164-168.

Lara, C., J. Fayyad, R. de Graaf, R. C. Kessler, S. Aguilar-Gaxiola, M. Angermeyer, K. Demytteneare, G. de Girolamo, J. M. Haro, R. Jin, E. G. Karam, J. P. Lépine, M. E. M. Mora, J. Ormel, J. Posada-Villa and N. Sampson (2009). "Childhood predictors of adult ADHD: Results from the WHO World Mental Health (WMH) Survey Initiative." <u>Biol Psychiatry</u> **65**(1): 46-54.

Lavenex, P. and D. G. Amaral (2000). "Hippocampal-neocortical interaction: a hierarchy of associativity." <u>Hippocampus</u> **10**(4): 420-430.

Leao, R. N., S. Mikulovic, K. E. Leao, H. Munguba, H. Gezelius, A. Enjin, K. Patra, A. Eriksson, L. M. Loew, A. B. Tort and K. Kullander (2012). "OLM interneurons differentially modulate CA3 and entorhinal inputs to hippocampal CA1 neurons." <u>Nat Neurosci</u> **15**(11): 1524-1530.

Lee, S. W. (1996). "H-cadherin, a novel cadherin with growth inhibitory functions and diminished expression in human breast cancer." <u>Nat Med</u> **2**(7): 776-782.

Lei, L. and L. Parada (2007). "Transcriptional regulation of Trk family neurotrophin receptors." <u>Cellular and molecular life sciences</u> **64**(5): 522-532.

Lesch, K. P., N. Timmesfeld, T. J. Renner, R. Halperin, C. Roser, T. T. Nguyen, D. W. Craig, J. Romanos, M. Heine, J. Meyer, C. Freitag, A. Warnke, M. Romanos, H. Schafer, S. Walitza, A. Reif, D. A. Stephan and C. Jacob (2008). "Molecular genetics of adult ADHD: converging evidence from genome-wide association and extended pedigree linkage studies." <u>J Neural Transm (Vienna)</u> **115**(11): 1573-1585.

Lesch, K. P. and J. Waider (2012). "Serotonin in the modulation of neural plasticity and networks: implications for neurodevelopmental disorders." <u>Neuron</u> **76**(1): 175-191.

Li, X., K. M. Rosborough, A. B. Friedman, W. Zhu and K. A. Roth (2007). "Regulation of mouse brain glycogen synthase kinase-3 by atypical antipsychotics." <u>Int J Neuropsychopharmacol</u> **10**(1): 7-19.

Li, Z., S. H. Chang, L. Y. Zhang, L. Gao and J. Wang (2014). "Molecular genetic studies of ADHD and its candidate genes: a review." <u>Psychiatry Res</u> **219**(1): 10-24.

Lorente de Nó, R. (1934). "Studies on the structure of the cerebral cortex. II. Continuation of the study of the ammonic system." <u>Journal für Psychologie und Neurologie</u>.

Lu, B. and W. Gottschalk (2000). Modulation of hippocampal synaptic transmission and plasticity by neurotrophins. <u>Progress in Brain Research</u>, Elsevier. **128:** 231-241.

MacArthur, J., E. Bowler, M. Cerezo, L. Gil, P. Hall, E. Hastings, H. Junkins, A. McMahon, A. Milano, J. Morales, Z. M. Pendlington, D. Welter, T. Burdett, L. Hindorff, P. Flicek, F. Cunningham and H. Parkinson (2017). "The new NHGRI-EBI Catalog of published genome-wide association studies (GWAS Catalog)." <u>Nucleic Acids Res</u> **45**(D1): D896-d901.

Marin, O. (2012). "Interneuron dysfunction in psychiatric disorders." <u>Nat Rev Neurosci</u> **13**(2): 107-120.

Martin, D. L. and K. Rimvall (1993). "Regulation of gamma-aminobutyric acid synthesis in the brain." <u>J Neurochem</u> **60**(2): 395-407.

Mendoza, J. E. and A. L. Foundas (2008). <u>Clinical neuroanatomy: a neurobehavioral approach</u>. New York, NY, Springer.

Minichiello, L. (2009). "TrkB signalling pathways in LTP and learning." <u>Nat Rev Neurosci</u> **10**(12): 850-860.

Minichiello, L., M. Korte, D. Wolfer, R. Kuhn, K. Unsicker, V. Cestari, C. Rossi-Arnaud, H. P. Lipp, T. Bonhoeffer and R. Klein (1999). "Essential role for TrkB receptors in hippocampus-mediated learning." <u>Neuron</u> **24**(2): 401-414.

Mizuno, M., K. Yamada, N. Takei, M. H. Tran, J. He, A. Nakajima, H. Nawa and T. Nabeshima (2003). "Phosphatidylinositol 3-kinase: a molecule mediating BDNF-dependent spatial memory formation." Mol Psychiatry **8**(2): 217-224.

Möhler, H. (2006). "GABA A receptors in central nervous system disease: anxiety, epilepsy, and insomnia." Journal of Receptors and Signal Transduction **26**(5-6): 731-740.

Morris, R. (1984). "Developments of a water-maze procedure for studying spatial learning in the rat." J Neurosci Methods **11**(1): 47-60.

Müller, C. and S. Remy (2014). "Dendritic inhibition mediated by O-LM and bistratified interneurons in the hippocampus." Frontiers in Synaptic Neuroscience **6**(23).

Nadel, L. and M. Moscovitch (1997). "Memory consolidation, retrograde amnesia and the hippocampal complex." Curr Opin Neurobiol **7**(2): 217-227.

Najarro, E. H., L. Wong, M. Zhen, E. P. Carpio, A. Goncharov, G. Garriga, E. A. Lundquist, Y. Jin and B. D. Ackley (2012). "The C. elegans Flamingo cadherin fmi-1 regulates GABAergic neuronal development." J Neurosci **32**(12): 4196-4211.

Nakazawa, K., V. Zsiros, Z. Jiang, K. Nakao, S. Kolata, S. Zhang and J. E. Belforte (2012). "GABAergic interneuron origin of schizophrenia pathophysiology." Neuropharmacology **62**(3): 1574-1583.

National Collaborating Centre for Mental Health (2009). National Institute for Health and Clinical Excellence: Guidance. Attention Deficit Hyperactivity Disorder: Diagnosis and Management of ADHD in Children, Young People and Adults. Leicester (UK), British Psychological Society (UK)
The British Psychological Society & The Royal College of Psychiatrists.

Neale, B. M., S. E. Medland, S. Ripke, P. Asherson, B. Franke, K. P. Lesch, S. V. Faraone, T. T. Nguyen, H. Schafer, P. Holmans, M. Daly, H. C. Steinhausen, C. Freitag, A. Reif, T. J. Renner, M. Romanos, J. Romanos, S. Walitza, A. Warnke, J. Meyer, H. Palmason, J. Buitelaar, A. A. Vasquez, N. Lambregts-Rommelse, M. Gill, R. J. Anney, K. Langely, M. O'Donovan, N. Williams, M. Owen, A. Thapar, L. Kent, J. Sergeant, H. Roeyers, E. Mick, J. Biederman, A. Doyle, S. Smalley, S. Loo, H. Hakonarson, J. Elia, A. Todorov, A. Miranda, F. Mulas, R. P. Ebstein, A. Rothenberger, T. Banaschewski, R. D. Oades, E. Sonuga-Barke, J. McGough, L. Nisenbaum, F. Middleton, X. Hu and S. Nelson (2010). "Meta-analysis of genome-wide association studies of attention-deficit/hyperactivity disorder." J Am Acad Child Adolesc Psychiatry **49**(9): 884-897.

Nobel Media AB. (2014). "The Nobel Prize in Physiology or Medicine 2007." Retrieved 28 Aug, 2017, from
https://www.nobelprize.org/nobel_prizes/medicine/laureates/2007/advanced.html.

Nollet, F., P. Kools and F. van Roy (2000). "Phylogenetic analysis of the cadherin superfamily allows identification of six major subfamilies besides several solitary members." J Mol Biol **299**(3): 551-572.

O'Keefe, J. and J. Dostrovsky (1971). "The hippocampus as a spatial map. Preliminary evidence from unit activity in the freely-moving rat." Brain Res **34**(1): 171-175.

O'Mara, S. M., S. Commins, M. Anderson and J. Gigg (2001). "The subiculum: a review of form, physiology and function." Prog Neurobiol **64**(2): 129-155.

Olfson, M., M. J. Gameroff, S. C. Marcus and P. S. Jensen (2003). "National trends in the treatment of attention deficit hyperactivity disorder." Am J Psychiatry **160**(6): 1071-1077.

Olsen, R. W., T. M. DeLorey, M. Gordey and M. H. Kang (1999). "GABA receptor function and epilepsy." Adv Neurol **79**: 499-510.

Paradis, S., D. B. Harrar, Y. Lin, A. C. Koon, J. L. Hauser, E. C. Griffith, L. Zhu, L. F. Brass, C. Chen and M. E. Greenberg (2007). "An RNAi-based approach identifies molecules required for glutamatergic and GABAergic synapse development." Neuron **53**(2): 217-232.

Pece, S. and J. S. Gutkind (2000). "Signaling from E-cadherins to the MAPK pathway by the recruitment and activation of epidermal growth factor receptors upon cell-cell contact formation." J Biol Chem **275**(52): 41227-41233.

Petroff, O. A. (2002). "Book review: GABA and glutamate in the human brain." The Neuroscientist **8**(6): 562-573.

Philippova, M., D. Ivanov, R. Allenspach, Y. Takuwa, P. Erne and T. Resink (2005). "RhoA and Rac mediate endothelial cell polarization and detachment induced by T-cadherin." Faseb j **19**(6): 588-590.

Philippova, M., D. Ivanov, M. B. Joshi, E. Kyriakakis, K. Rupp, T. Afonyushkin, V. Bochkov, P. Erne and T. J. Resink (2008). "Identification of proteins associating with glycosylphosphatidylinositol- anchored T-cadherin on the surface of vascular endothelial cells: role for Grp78/BiP in T-cadherin-dependent cell survival." Mol Cell Biol **28**(12): 4004-4017.

Philippova, M., D. Ivanov, V. Tkachuk, P. Erne and T. J. Resink (2003). "Polarisation of T-cadherin to the leading edge of migrating vascular cells in vitro: a function in vascular cell motility?" Histochemistry and Cell Biology **120**(5): 353-360.

Philippova, M., M. B. Joshi, E. Kyriakakis, D. Pfaff, P. Erne and T. J. Resink (2009). "A guide and guard: the many faces of T-cadherin." Cell Signal **21**(7): 1035-1044.

Polanczyk, G. V., E. G. Willcutt, G. A. Salum, C. Kieling and L. A. Rohde (2014). "ADHD prevalence estimates across three decades: an updated systematic review and meta-regression analysis." Int J Epidemiol **43**(2): 434-442.

Preilowski, B. (2009). "Erinnerung an einen Amnestiker (und ein halbes Jahrhundert Gedächtnisforschung)." Fortschr Neurol Psychiatr **77**(10): 568-576.

Raftopoulou, M. and A. Hall (2004). "Cell migration: Rho GTPases lead the way." Dev Biol **265**(1): 23-32.

Ramakers, C., J. M. Ruijter, R. H. Deprez and A. F. Moorman (2003). "Assumption-free analysis of quantitative real-time polymerase chain reaction (PCR) data." Neurosci Lett **339**(1): 62-66.

Ramamoorthi, K. and Y. Lin (2011). "The contribution of GABAergic dysfunction to neurodevelopmental disorders." Trends Mol Med **17**(8): 452-462.

Ramón y Cajal, S. (1893). Estructura del asta de Ammon y fascia dentata ; Estructura de la corteza occipital inferior de los pequeños mamíferos ; trabajos leidos ante la Sociedad Española de Historia Natural en la sesión del 5 de abril de 1893. Madrid, Establecimiento Tipográfico de Fortanet.

Ranscht, B. and M. T. Dours-Zimmermann (1991). "T-cadherin, a novel cadherin cell adhesion molecule in the nervous system lacks the conserved cytoplasmic region." Neuron **7**(3): 391-402.

Read, D. E. and A. M. Gorman (2009). "Involvement of Akt in neurite outgrowth." Cell Mol Life Sci **66**(18): 2975-2984.

Resink, T. J., M. Philippova, M. B. Joshi, E. Kyriakakis and P. Erne (2009). "Cadherins and cardiovascular disease." Swiss Med Wkly **139**(9-10): 122-134.

Risch, N. and K. Merikangas (1996). "The future of genetic studies of complex human diseases." Science **273**(5281): 1516-1517.

Rivero, O., M. M. Selten, S. Sich, S. Popp, L. Bacmeister, E. Amendola, M. Negwer, D. Schubert, F. Proft, D. Kiser, A. G. Schmitt, C. Gross, S. M. Kolk, T. Strekalova, D. van den Hove, T. J. Resink, N. Nadif Kasri and K. P. Lesch (2015). "Cadherin-13, a risk gene for ADHD and comorbid disorders, impacts GABAergic function in hippocampus and cognition." Transl Psychiatry **5**: e655.

Rivero, O., S. Sich, S. Popp, A. Schmitt, B. Franke and K. P. Lesch (2013). "Impact of the ADHD-susceptibility gene CDH13 on development and function of brain networks." Eur Neuropsychopharmacol **23**(6): 492-507.

Romanos, M., C. Freitag, C. Jacob, D. W. Craig, A. Dempfle, T. T. Nguyen, R. Halperin, S. Walitza, T. J. Renner, C. Seitz, J. Romanos, H. Palmason, A. Reif, M. Heine, C. Windemuth-Kieselbach, C. Vogler, J. Sigmund, A. Warnke, H. Schafer, J. Meyer, D. A. Stephan and K. P. Lesch (2008). "Genome-wide linkage analysis of ADHD using high-density SNP arrays: novel loci at 5q13.1 and 14q12." Mol Psychiatry **13**(5): 522-530.

Ruijter, J. M., C. Ramakers, W. M. Hoogaars, Y. Karlen, O. Bakker, M. J. van den Hoff and A. F. Moorman (2009). "Amplification efficiency: linking baseline and bias in the analysis of quantitative PCR data." Nucleic Acids Res **37**(6): e45.

Sauer, B. (1987). "Functional expression of the cre-lox site-specific recombination system in the yeast Saccharomyces cerevisiae." Mol Cell Biol **7**(6): 2087-2096.

Schiller, D., H. Eichenbaum, E. A. Buffalo, L. Davachi, D. J. Foster, S. Leutgeb and C. Ranganath (2015). "Memory and Space: Towards an Understanding of the Cognitive Map." J Neurosci **35**(41): 13904-13911.

Schür, R. R., L. W. Draisma, J. P. Wijnen, M. P. Boks, M. G. Koevoets, M. Joëls, D. W. Klomp, R. S. Kahn and C. H. Vinkers (2016). "Brain GABA levels across psychiatric disorders: A systematic literature review and meta‐analysis of 1H‐MRS studies." Human brain mapping **37**(9): 3337-3352.

Scoville, W. B. and B. Milner (1957). "Loss of recent memory after bilateral hippocampal lesions." J Neurol Neurosurg Psychiatry **20**(1): 11-21.

Sieghart, W. and G. Sperk (2002). "Subunit composition, distribution and function of GABA(A) receptor subtypes." Curr Top Med Chem **2**(8): 795-816.

Sik, A., M. Penttonen, A. Ylinen and G. Buzsaki (1995). "Hippocampal CA1 interneurons: an in vivo intracellular labeling study." J Neurosci **15**(10): 6651-6665.

Simon, V., P. Czobor, S. Balint, A. Meszaros and I. Bitter (2009). "Prevalence and correlates of adult attention-deficit hyperactivity disorder: meta-analysis." Br J Psychiatry **194**(3): 204-211.

Soghomonian, J. J. and D. L. Martin (1998). "Two isoforms of glutamate decarboxylase: why?" Trends Pharmacol Sci **19**(12): 500-505.

Somogyi, P. and T. Klausberger (2005). "Defined types of cortical interneurone structure space and spike timing in the hippocampus." J Physiol **562**(Pt 1): 9-26.

Sprich, S., J. Biederman, M. H. Crawford, E. Mundy and S. V. Faraone (2000). "Adoptive and biological families of children and adolescents with ADHD." J Am Acad Child Adolesc Psychiatry **39**(11): 1432-1437.

Squire, L. R. (2004). "Memory systems of the brain: a brief history and current perspective." Neurobiol Learn Mem **82**(3): 171-177.

Squire, L. R., C. E. Stark and R. E. Clark (2004). "The medial temporal lobe." Annu Rev Neurosci **27**: 279-306.

Stella, F., E. Cerasti, B. Si, K. Jezek and A. Treves (2012). "Self-organization of multiple spatial and context memories in the hippocampus." Neurosci Biobehav Rev **36**(7): 1609-1625.

Sterio, D. C. (1984). "The unbiased estimation of number and sizes of arbitrary particles using the disector." J Microsc **134**(Pt 2): 127-136.

Stranger, B. E., E. A. Stahl and T. Raj (2011). "Progress and Promise of Genome-Wide Association Studies for Human Complex Trait Genetics." Genetics **187**(2): 367-383.

Szabadics, J., C. Varga, G. Molnar, S. Olah, P. Barzo and G. Tamas (2006). "Excitatory effect of GABAergic axo-axonic cells in cortical microcircuits." Science **311**(5758): 233-235.

Takeichi, M. (2007). "The cadherin superfamily in neuronal connections and interactions." Nat Rev Neurosci **8**(1): 11-20.

Takeuchi, T., A. Misaki, S. B. Liang, A. Tachibana, N. Hayashi, H. Sonobe and Y. Ohtsuki (2000). "Expression of T-cadherin (CDH13, H-Cadherin) in human brain and its characteristics as a negative growth regulator of epidermal growth factor in neuroblastoma cells." J Neurochem **74**(4): 1489-1497.

Tovote, P., J. P. Fadok and A. Luthi (2015). "Neuronal circuits for fear and anxiety." Nat Rev Neurosci **16**(6): 317-331.

Toyoda, H., X.-Y. Li, L.-J. Wu, M.-G. Zhao, G. Descalzi, T. Chen, K. Koga and M. Zhuo (2011). "Interplay of Amygdala and Cingulate Plasticity in Emotional Fear." Neural Plasticity **2011**: 9.

Tricoire, L., K. A. Pelkey, B. E. Erkkila, B. W. Jeffries, X. Yuan and C. J. McBain (2011). "A blueprint for the spatiotemporal origins of mouse hippocampal interneuron diversity." J Neurosci **31**(30): 10948-10970.

Tyagarajan, S. K. and J.-M. Fritschy (2014). "Gephyrin: a master regulator of neuronal function?" Nature Reviews Neuroscience **15**(3): 141-156.

van Roy, F. and G. Berx (2008). "The cell-cell adhesion molecule E-cadherin." Cell Mol Life Sci **65**(23): 3756-3788.

Vaz, S. H., T. N. Jorgensen, S. Cristovao-Ferreira, S. Duflot, J. A. Ribeiro, U. Gether and A. M. Sebastiao (2011). "Brain-derived neurotrophic factor (BDNF) enhances GABA transport by modulating the trafficking of GABA transporter-1 (GAT-1) from the plasma membrane of rat cortical astrocytes." J Biol Chem **286**(47): 40464-40476.

Vullhorst, D., J. Neddens, I. Karavanova, L. Tricoire, R. S. Petralia, C. J. McBain and A. Buonanno (2009). "Selective expression of ErbB4 in interneurons, but not pyramidal cells, of the rodent hippocampus." J Neurosci **29**(39): 12255-12264.

Weibel, E. R., G. S. Kistler and W. F. Scherle (1966). "Practical stereological methods for morphometric cytology." J Cell Biol **30**(1): 23-38.

Wells, K. C., T. C. Chi, S. P. Hinshaw, J. N. Epstein, L. Pfiffner, M. Nebel-Schwalm, E. B. Owens, L. E. Arnold, H. B. Abikoff, C. K. Conners, G. R. Elliott, L. L. Greenhill, L. Hechtman, B. Hoza, P. S. Jensen, J. March, J. H. Newcorn, W. E. Pelham, J. B. Severe, J. Swanson, B. Vitiello and T. Wigal (2006). "Treatment-related changes in objectively measured parenting behaviors in the multimodal treatment study of children with attention-deficit/hyperactivity disorder." J Consult Clin Psychol **74**(4): 649-657.

West, A. E., E. C. Griffith and M. E. Greenberg (2002). "Regulation of transcription factors by neuronal activity." Nat Rev Neurosci **3**(12): 921-931.

West, M. J. (2012). "Estimating object number in biological structures." Cold Spring Harb Protoc **2012**(10): 1049-1066.

West, M. J. (2012). "Introduction to stereology." Cold Spring Harb Protoc **2012**(8).

West, M. J., L. Slomianka and H. J. Gundersen (1991). "Unbiased stereological estimation of the total number of neurons in thesubdivisions of the rat hippocampus using the optical fractionator." Anat Rec **231**(4): 482-497.

Wheelock, M. J. and K. R. Johnson (2003). "Cadherin-mediated cellular signaling." Curr Opin Cell Biol **15**(5): 509-514.

Williamson, D. and C. Johnston (2015). "Gender differences in adults with attention-deficit/hyperactivity disorder: A narrative review." Clin Psychol Rev **40**: 15-27.

Xu, B., W. Gottschalk, A. Chow, R. I. Wilson, E. Schnell, K. Zang, D. Wang, R. A. Nicoll, B. Lu and L. F. Reichardt (2000). "The role of brain-derived neurotrophic factor receptors in the mature hippocampus: modulation of long-term potentiation through a presynaptic mechanism involving TrkB." J Neurosci **20**(18): 6888-6897.

Yamada, K. and T. Nabeshima (2003). "Brain-derived neurotrophic factor/TrkB signaling in memory processes." J Pharmacol Sci **91**(4): 267-270.

Yamada, M. K., K. Nakanishi, S. Ohba, T. Nakamura, Y. Ikegaya, N. Nishiyama and N. Matsuki (2002). "Brain-derived neurotrophic factor promotes the maturation of GABAergic mechanisms in cultured hippocampal neurons." J Neurosci **22**(17): 7580-7585.

Yang, L., S. Chang, Q. Lu, Y. Zhang, Z. Wu, X. Sun, Q. Cao, Y. Qian, T. Jia, B. Xu, Q. Duan, Y. Li, K. Zhang, G. Schumann, D. Liu, J. Wang, Y. Wang and L. Lu (2017). "A new locus regulating MICALL2 expression was identified for association with executive inhibition in children with attention deficit hyperactivity disorder." Mol Psychiatry.

Zhang, L., S. Chang, Z. Li, K. Zhang, Y. Du, J. Ott and J. Wang (2012). "ADHDgene: a genetic database for attention deficit hyperactivity disorder." Nucleic Acids Res **40**(Database issue): D1003-1009.

Zhou, K., A. Dempfle, M. Arcos-Burgos, S. C. Bakker, T. Banaschewski, J. Biederman, J. Buitelaar, F. X. Castellanos, A. Doyle, R. P. Ebstein, J. Ekholm, P. Forabosco, B. Franke, C. Freitag, S. Friedel, M. Gill, J. Hebebrand, A. Hinney, C. Jacob, K. P. Lesch, S. K. Loo, F. Lopera, J. T. McCracken, J. J. McGough, J. Meyer, E. Mick, A. Miranda, M. Muenke, F. Mulas, S. F. Nelson, T. T. Nguyen, R. D. Oades, M. N. Ogdie, J. D. Palacio, D. Pineda, A. Reif, T. J. Renner, H. Roeyers, M. Romanos, A. Rothenberger, H. Schafer, J. Sergeant, R. J. Sinke, S. L. Smalley, E. Sonuga-Barke, H. C. Steinhausen, E. van der Meulen, S. Walitza, A. Warnke, C. M. Lewis, S. V. Faraone and P. Asherson (2008). "Meta-analysis of genome-wide linkage scans of attention deficit hyperactivity disorder." Am J Med Genet B Neuropsychiatr Genet **147b**(8): 1392-1398.

Zhu, M. and S. Zhao (2007). "Candidate Gene Identification Approach: Progress and Challenges." Int J Biol Sci **3**(7): 420-427.

5.3 Curriculum Vitae

5.4 Acknowledgements

5.5. Affidavit

I hereby confirm that my thesis entitled "Effect of Cadherin-13 inactivation on different GABAergic interneuron populations of the mouse hippocampus" is the result of my own work. I did not receive any help or support from commercial consultants. All sources and / or materials applied are listed and specified in the thesis.

Furthermore, I confirm that this thesis has not yet been submitted as part of another examination process neither in identical nor in similar form.

Place, Date   Signature

5.6 Eidesstattliche Erklärung

Hiermit erkläre ich an Eides statt, die Dissertation "Effect of Cadherin-13 inactivation on different GABAergic interneuron populations of the mouse hippocampus" eigenhändig, d.h. insbesondere selbständig und ohne Hilfe eines kommerziellen Promotionsberaters, angefertigt und keine anderen als die von mir angegebenen Quellen und Hilfsmittel verwendet zu haben.

Ich erkläre außerdem, dass die Dissertation weder in der gleichen noch in ähnlicher Form bereits in einem anderen Prüfungsverfahren vorgelegen hat.

Ort, Datum   Unterschrift